This is the post print version of the article, which has been published in AMERICAN JOURNAL OF SURGICAL PATHOLOGY. 2018, 42(1), 103-115.http://dx.doi.org/10.1097/PAS.0000000000000961

Feasibility of prostate PAXgene fixation for molecular research and diagnostic surgical pathology: Comparison of matched fresh frozen, FFPE and PFPE tissues.

Gunilla Högnäs, PhD,* Kati Kivinummi, PhD,* Heini M.L. Kallio PhD,* Reija Hieta, PhD,* Pekka Ruusuvuori, DSc,*□ Antti Koskenalho MS,* Juha Kesseli PhD,* Teuvo L.J. Tammela MD PhD,*† Jarno Riikonen MD PhD,† Joanna Ilvesaro, PhD,¶ Saara Kares,¶ Pasi P. Hirvikoski, MD PhD,# Marita Laurila, MD,¶ Tuomas Mirtti MD PhD,‡ Matti Nykter PhD,* Paula M. Kujala, MD,¶ Tapio Visakorpi, MD PhD,*¶ Teemu Tolonen, MD PhD,¶ and G. Steven Bova, MD,*

*Prostate Cancer Research Center, Faculty of Medicine and Life Sciences and BioMediTech Institute, University of Tampere, Tampere, FI-33014, Finland

□Tampere University of Technology, Pori, Finland.

†Department of Urology, University of Tampere, Tampere University Hospital, Tampere, Finland

¶Department of Pathology, Tampere University Hospital, Fimlab Laboratories, Tampere, Finland

#Department of Pathology, Oulu University Hospital, Oulu, Finland

‡Institute for Molecular Medicine Finland, University of Helsinki, Helsinki, Finland; Department of Pathology, HUSLAB, Helsinki University Hospital, Helsinki, Finland.

Correspondence to: G. S. Bova, University of Tampere, BioMediTech, P.O. Box 100, FI-33014 Tampere, Finland; g.steven.bova@uta.fi

Conflict of Interest: The authors declare no conflicts of interest.

Funding: Cancer Society of Finland, Academy of Finland, Finnish Cancer Institute, K. Albin Johansson Foundation, Finnish-Norwegian Medical Foundation

Keywords: prostate cancer; tissue processing; tissue fixation; histology; immunostaining; DNA quality; RNA quality; DNA yield; RNA yield; sequencing artifact; histomorphology; PAXgene; Formalin; FFPE; PFPE; fragment analyzer; RNA quality number; comparative study; frozen tissue; formalin-fixed tissue; paxgene-fixed tissue;

ABSTRACT

Advances in prostate cancer biology and diagnostics are dependent upon high fidelity integration of clinical, histomorphologic, and molecular phenotypic findings. In this study we compared fresh frozen (FF), formalin-fixed paraffin-embedded (FFPE), and PAXgene-fixed paraffin-embedded (PFPE) tissue preparation methods in radical prostatectomy prostate tissue from 36 patients and did a preliminary test of feasibility of using PFPE tissue in routine prostate surgical pathology diagnostic assessment. In addition to comparing histology, immunohistochemistry, and general measures of DNA and RNA integrity in each fixation method, we performed functional tests of DNA and RNA quality including targeted Miseq RNA and DNA sequencing, and implemented methods to relate DNA and RNA yield and quality to quantified DNA and RNA picogram nuclear content in each tissue volume studied. Our results suggest that it is feasible to use PFPE tissue for routine robot-assisted laparoscopic prostatectomy (RALP) surgical pathology diagnostics and immunohistochemistry, with the benefit of significantly improved DNA and RNA quality and RNA picogram yield per nucleus as compared to FFPE tissue. For FF, FFPE, and PFPE tissues respectively, average Genomic Quality Numbers (GQNs) were 7.9, 3.2, and 6.2, average RNA Quality Number (RQNs) were 8.7, 2.6, and 6.3, average DNA picogram yields per nucleus were 0.41, 0.69, and 0.78, and average RNA picogram yields per nucleus were 1.40, 0.94, and 2.24. These findings suggest that where DNA and/or RNA analysis of tissue is required, and when tissue size is small, PFPE may provide important advantages over FFPE. The results also suggest several interesting nuances including potential avenues to improve RNA quality in FFPE tissues, and confirm recent suggestions that some DNA sequence artifacts associated with FFPE can be avoided.

INTRODUCTION

Advances in prostate cancer biology and diagnostics are dependent upon high fidelity integration of clinical, histomorphologic, and molecular phenotypic findings. While frozen tissue can provide excellent molecular preservation, it is not suitable for routine surgical pathology as histologic detail is often insufficient, and frozen tissue handling is too cumbersome for routine analysis of entire prostates. Formalin-fixed, paraffin-embedded (FFPE) tissue processing, the current standard in surgical pathology, provides good histomorphology, but RNA and DNA isolated from FFPE tissue is significantly reduced both in overall yield and quality relative to frozen tissue.

PAXgene™ fixative (Preanalytix GmbH, Switzerland) is a non-crosslinking fixation reagent containing methanol and acetic acid (PAXgene Tissue Fix Container Circular). Studies have found PAXgene-fixed, paraffin-embedded (PFPE) tissue histology generally comparable to FFPE tissue in various tissue types[1–4]. However, depending on the epitope studied, immunohistochemistry (IHC) in PFPE tissue sections may require modification of IHC protocols originally optimized for FFPE[3,5]. Published comparative analysis of FFPE and PFPE prostate tissue is limited to a total of 13 cases from autopsy or surgery[1,3,6]. Prostate PFPE tissue histology has been reported to contain artifacts such as pyknosis of nuclei, cell shrinkage and lower contrast of the prostate epithelium compared to FFPE tissue in H&E stained specimens obtained at surgery[6]. Gillard et al reported RIN scores <2 in PFPE and FFPE material from apparently both autopsy and prostatectomy specimens, but no preanalytical tissue handling data was provided[1]. No study yet reported has directly compared fresh frozen (FF), FFPE, and PFPE molecular integrity and assessed general histologic quality in a blinded fashion in a substantial number of cases.

In this study we compared FF, FFPE, and PFPE tissue preservation methods for prostate tissue and did a preliminary test of feasibility of using PFPE tissue in routine prostate surgical pathology diagnostic assessment. We attempted to optimize every step of sample handling from robot-assisted laparoscopic prostatectomy surgery through processing, embedding, and storage of tissue blocks, with the intent of obtaining the best combination of histology and macromolecule quality for all three types of tissue studied (FF, FFPE, and PFPE). In addition to comparing histology, IHC, and general measures of DNA and RNA integrity in each fixation method, we performed functional tests of DNA and RNA quality, and implemented methods to relate DNA and RNA yield and quality to quantified nuclear content in each tissue volume studied.

MATERIALS AND METHODS

Study Design

We compared FF, FFPE and PFPE tissue quality in two phases (Fig. 1). In the first phase comprising tissue samples from 20 robot-assisted laparoscopic prostatectomy (RALP) cases herein referred to as the 4-core study, we compared FF, FFPE and PFPE results using two different tissue processors for PAXgene-fixed prostate tissue; a Shandon Citadel 2000

research histoprocessor and a Pathos Delta processor in use in surgical pathology (Fig. 1A). The RNA quality results in the 4-core study were less than desired (Supplemental Figure 1), compelling us to continue the study in a second phase using adjusted methods. The second phase (3-core study) comprised an additional 16 RALP cases where PAXgene fixed material was processed using a Leica TP1020 processor dedicated solely to PAXgene-fixed samples, and included use of reduced melting point paraffin (Fig. 1B). Methods and results for both phases of the study are reported here and summarized in Supplemental Table 1.

Tissue Collection and Sampling

Prostate tissue from robot-assisted laparoscopic prostatectomy (RALP) was used for the study. Consecutive cases from all surgeons performing RALP where tissue accrual coordinators (G.H., K.K., T.T.) were available were included in the study. Tissue used for the study remained available for routine diagnostic use.

RALP specimens were delivered from the operating room to surgical pathology (Fimlab, Laboratories, Tampere, Finland) by pneumatic tube in internally sterile specimen bags. Upon arrival, the prostate was immediately weighed in its bag and the prostate core temperature was measured with a sterile digital meat thermometer probe inserted to the midpoint of the prostatic urethra. Approximately 30 mL of Sterile 4°C saline solution was poured into the plastic bag containing the tissue to enhance heat transfer, the bag was covered with ice, and the prostate was cooled over 7-10 minutes to 15°C or below. The prostate was then inked for routine surgical pathology margin analysis (Supplemental Methods) and a 6 mm thick transverse tissue slice was cut midway between apex and base with a sterile custom-made tissue slicer. This tissue slice was placed on a sterile dissection plate with its apical side facing up. In the four-core study, four tissue core punches (A, B, C, and D) were taken with a sterile 8 mm diameter tissue biopsy punch (33-37-10, Miltex) clockwise along the anterior side of the prostate, each 3-4 mm away from the inked outer surface of the prostate as shown in Figure 1A to avoid risk of interfering with microscopic assessment of capsular margins. In the three-core study, three tissue core punches (A, B and C) were taken with a sterile 6 mm diameter tissue biopsy punch (33-36-10, Miltex), each 3-4 mm away from the inked outer surface of the posterolateral surface of the prostate as shown in Fig. 1B. In the 3-core study, the cores were taken from the left or right posterolateral position depending on the side most likely to contain cancer based on pre-operative biopsy results and pathologist's gross assessment of the tissue after slicing. Before removing the cores for fixation, the upward facing apical sides of each core were blue-inked to allow for correct orientation on

embedding. Core A was placed directly onto a cryomold and refrigerated OCT (Optimal Cutting Temperature; Sakura Finetek Europe B.V.) compound was placed around it. Core A was then snap frozen in -90°C isopentane for 15 seconds before storing it in -80ºC. Core B was placed in a labelled nylon mesh tissue bag (6774017, Thermo Scientific), fixed in 10% buffered Formalin (122256, Reagena International Oy Ltd) at least 24 hours, and processed in the next routine surgical pathology tissue processing run. Core C and D were placed in a labelled nylon mesh bag and fixed in 50 ml PAXgene fixative (Qiagen/PreAnalytix Cat No. 765312) for 4 hours at room temperature with gentle rocking (oscillating approximately once per minute). After fixation the C and D cores were transferred to 150 ml PAXgene Stabilizer diluted according to manufacturer instructions (Qiagen/PreAnalytix Cat. No. 765512) and stored at 4ºC until processing. After core sampling, the transverse prostate donor tissue slice was put into a Supa Mega Slim white cassette (CellPath, EAN 0102-02A) to reduce warping of the tissue during fixation and was placed in 10% buffered formalin.

Tissue Processing and Embedding

In both the 3-core and 4-core studies, the formalin-fixed B cores in nylon mesh bags were processed together with the whole mount prostate slice from which the cores were taken in a Pathos Delta processor as part of routine surgical pathology tissue processing at Fimlab (Supplemental Table 2). B cores were embedded in regular tissue cassettes in Histowax paraffin (melting point 56C-58C, Histolab), with the inked apical side as the initial cutting surface. In the 4-core study, the C and D cores were stored in Stabilizer solution at 4ºC between 16 hours to 20 days before processing, which was completed in three batches. The C cores were processed using newly replenished processing liquids in a fully cleaned Shandon Citadel 2000 research histoprocessor, and D cores were processed using replenished liquids in a fully cleaned Pathos Delta processor. C and D cores were embedded in Histowax in regular cassettes immediately upon processor run completion. In the 3-core study, the C cores were stored from 3 to 14 days in Stabilizer at 4ºC and were all processed in labeled nylon-mesh bags in one batch in a Leica TP1020 processor using Paraplast Xtra (melting point 50C-54C, P3808 Sigma-Aldrich) as embedding medium. Immediately upon processor run completion, C core tissues were removed from the wax chamber and embedded in Paraplast Xtra paraffin in regular cassettes. Detailed processing steps for the C and D cores in the two phases of the study are contained in Supplemental Tables 3-5. All study B, C, and D-core tissue blocks were stored at 4ºC when not being sectioned.

Tracking of Blocks, Slides, Tissue Reagents, Methods, and Results

All study blocks, slides, tissue reagents, images, methods, and results are tracked using unique identifiers and barcodes in a laboratory Integrated Life Science Research (ILSR) database.

Core Sectioning for H&E, IHC, and DNA/RNA Isolation

Consecutive tissue sections were cut from each core block for H&E (Hematoxylin and Eosin) staining, IHC and DNA/RNA extraction. For the paraffin-embedded B, C and D cores a 4 μm thick section was first cut with a microtome for H&E, followed by six 4 μm sections to be used for IHC staining. The slides were baked for 2 hours at 62.5ºC. After this, excess paraffin was trimmed away from the face of each block and 12 ten μm sections, comprising a tissue volume of 6.0 mm^3, or 22 ten μm sections, comprising a tissue volume of 6.2 mm^3, were cut from the 4-core study and 3-core study blocks, respectively. The tissue sections were placed into 1.5.ml Eppendorf tubes for DNA and RNA extraction (Fig. 2). For the A (frozen) cores, a 6 μm section was first cut with a cryotome for H&E staining, then excess OCT compound was removed before cutting 12 (4-core study) or 22 (3-core study) ten μm sections for nucleic acid extraction (Fig. 2).

Hematoxylin and Eosin Staining

In the 4-core study, four micron sections from B, C and D cores were stained by hand with the same H&E protocol optimized to give reasonably good quality staining in both FFPE and PFPE tissues (Supplemental Table 6). H&E staining of A core sections was done with a standard protocol for frozen sections (Supplemental Table 7). In the 3-core study, four micron sections from B cores were H&E stained at Fimlab pathology laboratory with an automated staining machine using their standard H&E protocol (Supplemental Table 8). To match the eosin staining intensity of the B cores as closely as possible, the PAXgene-fixed C cores were stained by hand using a modified protocol with diluted eosin and shorter eosin exposure time (Supplemental Table 9). Eosin concentration and time in eosin was reduced from 100% to 50% and 1 minute to 5 seconds respectively for PAXgene sections as compared to sections from formalin-fixed cores. The H&E staining protocol for frozen sections from A cores were similarly optimized to match staining intensities of formalin and PAXgene fixed sections (Supplemental Table 10).

Immunohistochemistry

Four micron sections from B, C and D cores for IHC were placed on either SuperFrost plus slides (PSA, ERG, Vimentin stains) or TOMO slides (Matsunami glass Ind., Ltd) (2IHC stain) using automated Bond III technology (PSA, ERG and Vimentin) or Ventana Benchmark GX technology ("2IHC" CK5/6, p63 and AMACR cocktail) (Fimlab) (detailed protocol in Supplemental Methods). The IHC sections were counterstained with hematoxylin. Overall immunohistochemistry results were compared for each trio of BCD IHC sections (4-core study) or BC IHC sections (3-core study) by two pathologists (T.T. and G.S.B.).

Whole Slide Imaging

H&E and IHC whole slide images in the 4-core study were obtained at 40x magnification with an Olympus BX51, Olympus UplanSApo 40x objective and Surveyor Software, Objective Imaging Ltd., and in the 3-core study with a Hamamatsu Photonics Nano Zoomer XR C12000 automated scanner. QC on whole slide images was done by visual inspection of the slides to make sure all images were in focus.

Surgical Pathologist Web-Based Survey

Five surgical pathologists (T.T., T.M., P.H., M.L., and P.K.) participated in a web-based survey including histologic images from study PFPE and FFPE tissue cores, from sections adjacent to those used for DNA and RNA isolation and analysis. Survey instructions and the specific questions used are contained in Supplemental Methods. For each of 14 FFPE and 19 PFPE blocks from the 3-core and 4-core studies containing cancer, paired H&E and 2IHC (AMACR, p63 and CK 5/6) stained section zoomable whole slide images were presented in randomized order to the pathologists at a computer of their choice. Pathologists were blinded to the case number, core identity, and fixative for each pair of images presented. For each pair of images, the pathologist was required to make a best estimate of what fixative was used (PAXgene or Formalin) and was required to choose whether or not the quality appeared adequate for routine radical prostatectomy surgical pathology analysis.

Nucleic Acid Extraction and Quality Assessment

Genomic DNA and total RNA, including miRNA, was extracted from all cores. Different column based extraction kits from Qiagen (Hilden, Germany) were used to isolate nucleic acids from the different tissue preparations as recommended by the manufacturer. AllPrep DNA/RNA/miRNA Universal kit (Qiagen, cat no 80224) was used for simultaneous extraction of DNA and RNA from the fresh frozen A cores and the Allprep DNA/RNA FFPE

kit (Qiagen, cat no 80234) was used for the formalin-fixed B cores. For the PAXgene-fixed C and D cores DNA and RNA was extracted with the PAXgene Tissue Allprep DNA/RNA/miRNA method (Qiagen's PX10 Supplemental protocol) where material from the PAXgene Tissue DNA Kit (Qiagen/PreAnalytix cat no 767134) and PAXgene Tissue miRNA Kit (Qiagen/PreAnalytix, cat no 766134) were used. The extractions were performed according to the manufacturer's instructions apart from modification of the deparaffinization protocols (details in Supplemental Methods). In brief, deparaffinization of 3-core study B core sections and 4-core study B, C and D core sections was performed by incubating the samples for 20 min at 37ºC with 1400 µl heptane, and deparaffinization of 3-core study C core sections was performed by incubating the samples for 10 minutes at room temperature with 650 µl xylene. The cut sections were stored in -80ºC and extractions were performed within two weeks after cutting. 60 µl of DNA and 40 µl of RNA was isolated and the eluted samples were stored at -20ºC and -80ºC, respectively.

DNA concentration was measured with the Qubit 2.0 Fluorometer (Invitrogen Life Technologies, Carlsbad, CA). Genomic DNA was run on a 0.6% agarose gel stained with 0.5x SYBR Safe DNA dye (Invitrogen) at 80V for 70 minutes and DNA band size examined under UV-light. DNA quality and RNA concentration and quality was measured with Fragment Analyzer (FA) (Advanced Analytical Technologies, Ankeny, IA) using the DNF-467 Genomic DNA 50kb Analysis kit and the DNF-489 Standard Sensitivity RNA Analysis kit. The results were analyzed with Fragment Analyzer PROsize 2.0 version 2.0.0.51 software. PROsize determines a Genomic Quality Number (GQN) based on relative quantity of genomic DNA above a user-defined 10 kb size threshold. When analyzing RNA, PROsize determines the percentage of RNA over 200 nucleotides in size (DV_{200}) and an RNA Quality Number (RQN) value based on the area and ratios of the 18S and 28S ribosomal RNA peaks. DV_{200} >70% is considered high quality and 30-50% low quality RNA for Illumina's (Illumina, San Diego, CA) RNA Seq library preparation[7]. According to Advanced Analytical Technologies, Fragment Analyzer RQN number and Agilent 2100 Bioanalyzer (Agilent Technologies, Santa Clara, CA) RIN number measured in comparison RNA samples are highly correlated (R^2= 0.9635)[8].

For the 3-core study samples, DNA quality of FF, FFPE and PFPE DNA was also analyzed with a qPCR (real time quantitative Polymerase Chain Reaction)-based FFPE QC kit (Illumina Kit WG-321-1001). This method compares the Ct (threshold cycle) of amplification

for control template and experimental DNA samples; a ΔCt value (Sample DNA Ct minus QC Template DNA Ct) of ≤ 2 is considered good quality DNA. Extracted DNA was diluted to 1 ng/µl and run in triplicate according to manufacturer's instructions.

Manual and Automated Nucleus Counts

Nucleus counts were obtained from the H&E stained face section whole slide images of A, B and C cores in the 3-core study using an automated nucleus counting method. All hematoxylin stained nuclei were manually counted from one 550 µm x 550 µm image randomly selected from every A, B and C core whole slide image, resulting to a total of 71239 manually annotated nuclei. Manual counting was done using the Cell Counter plugin in Image J software (v. 1.48, National Institutes of Health, Bethesda, MD), and coordinates with the position of each manually counted nucleus was saved for optimization of the automated counting method. Nucleus segmentation was done for color adjusted images. We used a histogram matching method for color adjustment, using a composite image histogram as a reference for the matching of red, green and blue channels. Nucleus segmentation was done in two passes. First, a smoothened pixelwise ratio image between red and blue channels was binarized using an experimentally defined threshold value. Second, any undersegmented connected components (larger than twice of the area of a typical nucleus) were thresholded using another threshold and the remaining large objects were further split using marker controlled watershed segmentation. Detected areas smaller than 4 μm^2 were cleaned from the results by applying area constraints. Finally, small bleed-through areas of blue ink used for external marking of correct orientation of the core were excluded by applying hue and saturation based thresholding as criteria. All parameters were tuned by using the manually counted cells as a validation set. The accuracy of segmentation was determined for the 71239 annotated cells as an F1-score, weighting both false positive and false negative errors equally. The average F1-score among the annotated images, defined as 2*precision*recall/(precision + recall)[9] was 0.78. Average precision (TP/(TP+ FP) was 0.85 and recall (TP/TP+FN) 0.73, where TP, FP are true and false positive detections, respectively, and FN denotes false negatives.

Per-Nucleus DNA and RNA Yield Estimation

Total nuclear count from all sections used for nucleic acid isolation was estimated based on the number of nuclei present in the adjacent H&E section from each core (see Fig 2), the thickness of tissue taken for DNA/RNA extraction and the median nuclear diameter. Median diameter was calculated for all segmented nuclei in A, B and C core images by assuming

spheroid shape with diameters estimated from segmented nuclei as axes of ellipsoid with equivalent normalized second order moments as the segmented nucleus area. The quotient of the total tissue thickness divided by the major axis of the cell nuclei was calculated for each core tissue section group used for DNA and RNA extraction. The nuclear count from the H&E section was then multiplied by this number to obtain the estimated total nuclear count in the tissue taken for extraction. For A cores this multiplication factor was 38.6 (220 µm/5.7 µm), for B and C cores it was 40.7 (220 µm/5.4 µm).

Cases Selected for DNA and RNA sequencing assay

DNA and RNA isolated from A, B, and C cores from four 3-core study cases were selected for Miseq-based sequence analysis based on C Core (PAXgene) RQN values in an attempt to get a picture of the range of sequencing performance to be expected from PAXgene fixed prostate tissues. We studied two cases with the lowest recorded average RQN (PAX 84 and 85, average RQNs 6 and 5.5 in two separate FA runs), and two cases with the highest recorded RQNs (PAX 91 and 96, average RQNs 6.7 and 6.9 respectively).

36-gene targeted Miseq DNA sequencing assay

AR and 35 other genes were targeted for capture and DNA sequencing (Supplemental Table 11) in DNA isolated from A, B, and C cores in the 3-core study. Targeted sequence enrichment was performed using the SureSelect^{XT} Target Enrichment System (Agilent Technologies, Santa Clara, CA) according to manufacturer's instructions. Briefly, 200 ng of genomic DNA was sheared using a Covaris instrument (Covaris, Woburn, MA) to yield a fragment size of 150-200 bp. End repair, addition of the 3'-dA overhang, ligation of indexing-specific adaptors, hybridization to custom RNA baits, hybrid capture selection and index tagging were performed according to the Illumina paired-end sequencing library protocol. All recommended quality control steps were performed between steps. The multiplexed samples were sequenced on the Illumina Miseq platform using 150 bp paired-end reads.

22-transcript targeted RNA sequencing assay

A custom RNA sequencing panel was designed to cover all *AR* exons and introns to enable investigation of most common *AR* splice variants; 21 other gene transcripts were also included (Supplemental Table 12). Targeted sequence enrichment was performed using the SureSelect^{XT} RNA Target Enrichment System (Agilent Technologies) according to manufacturer's instructions. Briefly, poly(A) RNA was purified from 1 µg of total RNA and

fragmented chemically. In the following steps, samples were prepared using SureSelect Strand-Specific RNA Library Prep Kit to obtain adaptor-ligated cDNA library amplicons. Finally, hybridization to custom RNA baits, hybrid capture selection and index tagging were performed. All the AMPure XP bead purification steps were conducted as instructed. The multiplexed samples were sequenced on the Illumina Miseq platform using 150 bp paired-end reads. In five samples with RQN <6, (one C core with RQN 5.5, and four B core samples) modifications were made to the protocol as recommended by Agilent Technologies: 1) Instead of poly(A) RNA purification from 1 µg total RNA, Ribo-Zero Gold Magnetic Kit (Illumina, San Diego, CA) was used to remove rRNA from 2 µg of total RNA. 2) Instead of fragmenting the purified RNA at 94ºC for 8 min, RNA was denatured at 65ºC for 5 min. 3) All AMPure XP bead purification steps were performed using 1.8:1 bead volume to sample volume ratio. 4) Instead of 13 cycles in the pre-capture PCR, the number of cycles was increased to 14.

DNA and RNA Sequence Analysis

RNA-seq reads were aligned to human genome assembly GRCh37.2 (hg19) using Tophat2, version 2.0.13[10]. RNA sequencing coverage was computed using BedTools, version 2.26.0[11]. For DNA damage analysis, DNA-seq reads were aligned to human genome assembly GRCh37.2 (hg19) using bowtie2, version 2.2.4[12]. Duplicates were removed from DNA-seq alignments using samblaster tool, version 0.1.22[13]. SAMTools mpileup, version 1.3.1[14] was used for generating a pileup output of the alignments. Discrepancies used for the calculation of the single nucleotide changes (SNCs) were determined by parsing the number and identity of the bases corresponding to a particular position from the output using custom R scripts. Only high quality alignments with mapping quality score > 20 were used for the analysis. To identify sequence artifacts, positions with variant allele frequency > 10% were excluded to minimize the number of true variants detected. In addition, positions with variant allele frequency < 1% were excluded as they were assumed to be sequencing errors. The frequency of each type of SNC was calculated by dividing the count of a given SNC by the total amount of the corresponding reference base calls and multiplying the result by 10^6.

Statistics

Quantitative differences between FF, FFPE and PFPE sample groups in the 3-core study were calculated using GraphPad software and groups were compared for statistical significance ($P<0.05$) using the unpaired t-test with Welch's correction (GraphPad PRISM, version 5.02, GraphPad Software). The comparisons of PFPE RQN values in 4-core and 3-core study

groups (Supplemental Figure 1) were tested for significance using the two-tailed Wilcoxon rank-sum test with Gaussian approximation for p-value calculation to break ties in the data.

RESULTS

Clinical Data

A standard set of intravenous drugs were used for anesthesia during RALP surgery (Supplemental Table 1). RALP pathology including Gleason grade and stage are contained in Supplemental Table 1.

Tissue Quality Related Times and Temperatures

Interval times and temperatures are compared for the 4-core and 3-core studies in Table 1. There are significant differences between the two studies in total prostate cooling time, total time from removal of the tissue from body to time in fixative, total time from patient under anesthesia to time in fixative and total time from first artery ligation to time in fixative (Table 1).

Tissue Cancer Cell Fraction

Cancer cell fraction (CCF) was visually estimated based on a H&E face section whole slide image from each core by one pathologist (G.S.B.). In FF, FFPE, and PFPE cores, average (range in parentheses) CCF was 11 (0-50), 19 (0-80), and 8 (0-62) respectively. Welch test showed no significant difference in average CCF in the three types of tissue studied.

Immunohistochemistry Overview

Comparison of B, C and D (4-core study only) core PSA, ERG, Vimentin and 2IHC stains from the 3-core and 4-core studies were performed by two pathologists (T.T. and G.S.B). The staining protocols used for B, C, and D core sections were identical, no changes were made in the standard Fimlab clinical staining methods (Supplemental Methods). For these four IHC stains, no systematic difference in quality was detected, and all stain results appeared adequate for routine use.

Surgical Pathologist Survey of H&E and 2IHC Histomorphology

Overall, among the 5 surgical pathologists, the rate of correct identification of the fixative used based on the paired H&E and 2IHC image survey averaged 64% and 45% for tissue sections from FFPE and PFPE material respectively. The four pathologists with little or no previous experience comparing histology from FFPE and PFPE prostate material were essentially not able to reliably discern the fixative purely from the side by side H&E and

2IHC whole-slide images. The one surgical pathologist in the group with extensive prior experience comparing PAXgene and formalin-fixed prostate tissue histology side by side (T.T.) was significantly better at identifying fixative from histology, identifying 13/14 of the formalin fixed blocks correctly and 15/16 of the PAXgene fixed blocks correctly. In the survey, this pathologist noted that identification was mainly by red blood cell morphology (Supplemental Figure 2) and by a tendency to excess hematoxylin staining in cases he identified as PAXgene-fixed.

Among the 5 pathologists, rated adequacy of the material for routine surgical pathology analysis was 100% and 96% for the FFPE and PFPE material respectively. One pathologist considered three of 16 PAXgene paired images inadequate for routine surgical pathology analysis, based on the carcinoma being partially AMACR negative in one case, and hyperchromasia being so intense in two cases that nucleoli were not visible. The other 4 pathologists considered all PAXgene H&E and 2IHC images adequate for routine surgical pathology. Representative examples of H&E and 2IHC staining in two cases where both FFPE and PFPE cores contained cancer are shown (Fig. 3, Supplemental Figure 3).

No differences were detected in the overall quality of the H&E and 2IHC data in the 4-core and 3-core study material included in the survey.

Nucleus Counts

In the 3-core study, average nucleus counts per standard slide for each type of tissue were 79839, 98609 and 86892 for FF (A), FFPE (B) and PFPE (C) cores, respectively. The counts were obtained by applying area and red/blue intensity based scaling to the counts given by nucleus detection. The correction factors used in scaling removed differences in average tissue areas and staining intensities between FF, FFPE,and PFPE cores. The total estimated nucleus count per 6.2 mm^3 tissue volume was 3.1×10^6, 4.0×10^6 and 3.5×10^6 for FF (A), FFPE (B) and PFPE (C) cores, respectively (Supplemental Table 13).

DNA Quality and Yield

DNA isolated from FF, FFPE, and PFPE varied significantly in quality. In the 3-core study, average GQN for FF (A Core), FFPE (B Core), and PFPE (C Core) material was 7.9, 3.2, and 6.2 respectively (all differences significant by Welch test $p<0.0001$, Fig. 4A). Average DNA fragment sizes for 3-core study A, B and C cores were 59, 20 and 41 kb respectively (Table 2, Supplemental Figures 4A and 5A). The overall pattern of DNA quality differences between FF, FFPE, and PFPE material is illustrated in Figure 4B, where representative

Fragment Analyzer electropherogram tracings are superimposed on the same axis, and by comparing the results of running aliquots of the DNA from all 3-core cases on an agarose gel (Supplemental Figure 4A). Both FF and PFPE DNA populations are largely contained in bell-shaped curves centered around the average, whereas FFPE DNA is notable for two peaks, one low 300 bp peak (about the length of DNA around two nucleosomes), and a larger peak at 20 kb. DNA quality results were similar in the 4-core study material (Supplemental Table 1, Supplemental Figure 4B).

Functional DNA quality of the 3-core study material was analyzed by Illumina FFPE QC assay. This method compares the qPCR Ct (threshold cycle) values between the analyzed samples and a reference DNA template. Average delta Ct values for FF (A Core), FFPE (B Core), and PFPE (C Core) material were -0.7, 1.9, and -0.6 respectively (Fig. 4C). FF and PFPE DNA performed similarly in this assay, while FFPE DNA performed significantly worse than either FF or PFPE DNA (Welch test, $p< 0.0001$).

In the Miseq DNA assay, similar read counts were obtained for 3-core study FF, FFPE, and PFPE DNA. We compared rates of sequence artifact in FF, FFPE, and PFPE DNA. With the exception of a disproportional increase of C>A changes in two of the four FFPE-derived samples, the rate of various other artifacts is similar among the three sample types (Supplemental Figure 5B).

Total DNA yield from unit volumes of FF, FFPE, and PFPE also varied significantly. In the 3-core study, average DNA yield from our standard 6.2 mm^3 tissue volume from FF (A Core), FFPE (B Core), and PFPE (C Core) material averaged 1.3 µg, 2.8 µg and 2.7 µg respectively. DNA yield from FF material was significantly lower than FFPE and PFPE (Welch test, $p<0.001$ and $p<0.01$, respectively), and total DNA yields for FFPE and PFPE material were nearly identical (Supplemental Figure 5C).

Using the estimated total nuclear count derived from image analysis of face sections from each core sample 6.2 mm^3 tissue volume, FF (A Core), FFPE (B Core), and PFPE (C Core) average DNA yield per nucleus was 0.41 pg (picogram), 0.69 pg and 0.78 pg respectively (Fig 4D). Variation in yield per nucleus within each of the three (FF, FFPE, and PFPE) sample types was low for FF samples, and higher for FFPE and PFPE samples.

RNA Quality and Yield

Total RNA isolated from FF, FFPE, and PFPE varied significantly in quality. Overall RNA quality features from A, B and C core tissues in the 3-core study are summarized in Table 2. In the 4-core study, average RQN for A, B, C core (PFPE processed in Citadel research processor) and D core (PFPE processed in Fimlab Pathos processor), were 9.1, 2.8, 4.6 and 5.1 respectively (Supplemental Table 1). In the 3-core study, average RQN for FF (A Core), FFPE (B Core), and PFPE (C Core) material was 8.7, 2.6, and 6.3 respectively (all differences significant by Welch test $p<0.0001$, Fig. 5A). RQN values from the PAXgene-fixed C cores inversely correlated with the time the cores sat in Stabilizer before processing ($R= -0.75$, $p<0.001$). There was no correlation between the 3-core study RQN or GQN values from matched FF, FFPE and PFPE cores (Supplemental Figure 6A). In addition, the RNA DV_{200} values (the percentage of RNA over 200 nucleotides in size) for FF, FFPE and PFPE cores were 81%, 50% and 76%, respectively (Table 2). The overall pattern of RNA quality differences between FF, FFPE, and PFPE material is illustrated in Figure 5B, where representative Fragment Analyzer electropherogram tracings are superimposed on the same axis. FF RNA contains sharp 18S (2 kb) and 28S (5 kb) ribosomal RNA peaks, PFPE RNA also shows a similar 18S peak and a 28S peak lower in amplitude. FFPE RNA 18S and 28S peaks are not discernible in this tracing.

Targeted sequencing of RNA transcripts showed decreased performance of FFPE RNA. While the mean total number of reads was similar in the three fixation groups ($>2.5x10^6$), the FFPE (B core) samples had a lower distribution of raw coverage at each position of target transcripts compared to both FF (A core) and PFPE (C core) samples (Fig. 5C). Comparing all 3-core study RNA samples, we found strong correlation between RQN values and median coverage ($R= 0.87$, $p<0.001$, Pearson correlation test).

Total RNA yield from unit volumes of FF, FFPE, and PFPE varied significantly. In the 3-core study, average RNA yield from our standard 6.2 mm^3 tissue volume from FF (A Core), FFPE (B Core), and PFPE (C Core) material averaged 4.3 µg, 3.7 µg and 7.8 µg respectively. RNA yield from PFPE material is significantly higher than for FFPE or FF material (Welch test, $p=0.0002$, $p=0.0005$, respectively), and total RNA yields for FF and FFPE material are not significantly different (Welch test, $p=0.39$, Supplemental Figure 6B).

In the 3-core study, using the estimated total nuclear count derived from image analysis of face sections from each core sample 6.2 mm^3 tissue volume, FF (A Core), FFPE (B Core), and PFPE (C Core) average RNA yield per nucleus was 1.40 pg, 0.94 pg and 2.24 pg respectively (Fig 5D).

Materials and Storage Costs

The average prostate weight in the combined 4-core and 3-core studies was 55.6 g. Qiagen recommends a ratio of tissue volume to PAXgene fixative volume of "at least 1:10" (Qiagen PAXgene Tissue Fix Product Circular). Most recent costs in our locality for 600 mL PAXgene fixative (170 €/190 USD) and 600 mL diluted PAXgene stabilizer (27 €/30 USD) are 18x higher than our local cost for 600 mL of Formalin (11 €/12 USD). Our local cost for equal 3kg of Paraplast Xtra paraffin (120 €/134 USD) is more than 6x higher than cost for the same amount of Histowax (18 €/20 USD), the standard paraffin used in Fimlab. In addition to materials costs, storage costs for PFPE tissues are higher, since they must be stored at 4°C or below to reduce degradation of biomolecule quality (Qiagen PAXgene Tissue Fix Product Circular).

DISCUSSION

Comparative analysis of Fresh Frozen, FFPE, and PFPE tissue sample histology, IHC, DNA and RNA quality from 36 prostatectomy specimens suggests that it is feasible to use PAXgene fixation and processing of prostate tissue for combined molecular research and diagnostic surgical pathology. PFPE tissues collected and processed under conditions similar to those in the second (3-core) phase of the study reported here will provide significantly better DNA and RNA quality and yield as compared to FFPE tissues, therefore providing support for tighter linkage between histomorphology and molecular genetic analysis of prostate cancer phenotypes, while providing sufficient quality histology for standard surgical pathology radical prostatectomy diagnostics.

The PFPE RNA quality obtained in the 3-core study (16 patients, average RQN 6.3) was significantly better than what was obtained in the initial 4-core study (20 patients, average RQN 5.1). In the 3-core study, a new dedicated tissue processor (Leica TP1020), lower melting point paraffin (ParaplastXtra) and a different deparaffinization method (Xylene at Room Temp) was used. Further study is needed to determine which of these three changes are most important to obtaining improved RNA quality. Another factor could be the

significantly reduced time to fixative, surgical time, and post-arterial ligation times (Table 1) in the 3-core cohort (improvements that were detected after the study and not specifically attempted). However, RNA quality in the FF tissues from the 4-core (average RQN 9.1) and 3-core cohort (average RQN 8.7) were not statistically significantly different, and therefore the RNA quality upon arrival in surgical pathology was already at a similar maximum in the 4-core study. Improvements in downstream RNA quality in the 3-core study are more likely due to some or all of the downstream changes specific to the 3-core study.

To our knowledge, this is the first study to compare DNA and RNA yield per nucleus using different processing methods. Surprisingly, we found that DNA yield per nucleus in FFPE (0.69 pg) and PFPE (0.78 pg) is similar (although FFPE DNA is markedly degraded compared to PFPE DNA), and DNA yield per nucleus from FF tissue using similar column-based extraction methods is significantly lower (0.41 pg) than both PFPE and FFPE. Why DNA yield per nucleus is lower in FF tissue is not clear. Differences in the column-based extraction protocols could account for some of these differences, but they are similar in their basic components and unfortunately are not open to scientific analysis since the content of the various solutions is not provided by Qiagen. A normal diploid human male cell is calculated to contain 6.1 pg of nuclear DNA[15]. Mitochondrial DNA is an important component of cellular DNA content, but contributes less than 1% of the total weight of DNA per cell[16,17]. Cancer nuclei are often aneuploid (with >6.1 pg of DNA per nucleus), but average cancer cell fraction among the three core types was similar. Our study therefore shows that the typical column-based extraction methods used here yield no more than 15% of the DNA available in the tissue. There is substantial room for DNA yield improvement, and we advocate using yield per nucleus in future DNA and RNA extraction studies to identify improvements.

The RNA yield (quantity) per nucleus was 1.40 pg with FF, 0.94 pg with FFPE, and 2.24 pg with PFPE. Surprisingly, PFPE provided better yield per nucleus than either FF or FFPE tissues. We detected no significant difference in cancer or other cell content in the A, B, and C cores, and therefore we do not think these differences are due to different cellular makeup among FF, FFPE, and PFPE cores. Why PFPE provided significantly greater RNA yield per nucleus than FF or FFPE tissue is not clear and if this is confirmed in future studies, could provide a rationale for preferred use of PAXgene processing of prostate biopsy material where cancer cell nuclei for molecular analysis are often relatively low in number.

In terms of quality, we found that PFPE DNA and RNA quality is significantly better than FFPE DNA and RNA quality, but also worse than DNA and RNA quality from FF tissue. Further tweaking of PFPE processing methods could yield even more intact DNA and RNA. A first step could be to isolate DNA from tissue fixed in PAXgene but not paraffin embedded. This could isolate whether PAXgene acetic acid causes strand breaks, or whether strand breaks occur during the heating and paraffin diffusion during processing and embedding or during paraffin extraction, or both.

Our results unexpectedly suggest how RNA quality routinely obtained from FFPE tissue could theoretically be markedly improved. Average FFPE RQN obtained in the 3-core study was only 2.6, but it ranged widely, from 1.1 to 5.4 (Supplemental Figure 6A), while RQN in FF and PFPE tissue from the same prostates were relatively stable. The FFPE tissues processed in the 3-core study were part of the regular surgical pathology workflow, meaning that while the tissues all contained RNA of high quality to start with and processing chemicals and times were similar among all FFPE blocks, the time the blocks sat in formalin prior to processing and in the processor at elevated temperature at the end of processing but before embedding, and the time maintained at elevated temperature during embedding likely varied substantially from case to case since this is currently not standardized. A controlled study comparing prostate RNA quality in tissues exposed to variable time in formalin and variable time in molten paraffin during embedding would test this hypothesis, and if true, average RNA quality in FFPE could be elevated to the RQN 4-5 range if surgical pathology routines can be modified to obtain the identified optimal times.

Reports of DNA sequence artifacts associated with formalin fixation[18] prompted us to compare sequence artifacts in matched FF, FFPE, and PFPE samples from four cases. Sequence from FF and PFPE shared a similar low rate of artifacts (Supplemental Figure 5B), another positive point for PFPE. Surprisingly, FFPE material from this study did not contain an excess of C>T transitions as found in 42-100% of samples in several prior studies[18] but two of the four FFPE samples did show an excess of C>A transversion artifacts of unknown origin. C>A artifacts were reported by Costello et al[19] to be associated with oxidation of DNA by acoustic shearing, a standard step prior to high throughput sequencing. In our study acoustic shearing was performed using standard settings for all DNA samples sequenced (from FF, FFPE, and PFPE tissues), so this is not likely the source of this artifact in our study. Moreover the C>A artifacts observed in the current study did not occur in the

CCG>CAG context reported by Costello et al[19]. The lack of excess of C>T base transitions detected in FFPE DNA in the current study, consistent with previous reports where such artifacts are less commonly found in tissues fixed in buffered formalin less than 72 hours and in younger tissue blocks[20,21], also supports the idea that such artifacts could be routinely minimized with better standardization of FFPE processing. However, we should add that excess C>T artifacts may have been present in the FFPE DNA, but not detected by our assay. FFPE DNA C>T base transitions are often caused by deamination of cytosine, leading to formation of uracil and the subsequent incorporation of an adenine base in the opposite strand. Some DNA polymerases recognize deaminated cytosine residues and stall amplification until the correct base is incorporated, thus preventing amplification of strands containing this artifact[22]. The ability of the Herculase II polymerase used in our sequencing assay to recognize deaminated bases is thus an additional possible reason for the low number of C>T artifacts detected in these FFPE samples[23].

There are nuances and limitations of the study worth mentioning. This study compared histology and IHC between matched FFPE and PFPE tissues only at a general level, it did not compare ability to do Gleason grading or surgical margin status determination. Five surgical pathologists reviewing paired H&E and 2IHC stained whole slide images in a blinded fashion rated 100% of FFPE material and 96% of PFPE material adequate for diagnostic surgical pathology. Comparison of Gleason grading and nuclear morphology was not performed in the current study because the comparison tissues were not sufficiently close to each other. Future studies could include “kissing” sections (one FFPE, one PFPE) to allow reasonably sound Gleason grading comparisons. Analysis of surgical margin status in surgical pathology laboratories where whole prostates are initially fixed overnight in formalin is quite different from analysis of surgical margins in prostates that are fully sectioned fresh, just after inking, as they must be to obtain high quality RNA with PAXgene fixation. This could also potentially be addressed in future studies by comparing margin status in “kissing” sections only microns apart.

In order to scientifically compare histologic adequacy of paired FFPE and PFPE material in future studies, H&E staining for PFPE sections should be adjusted to match standard H&E staining in FFPE tissue sections. In the current study, in PFPE tissue sections, a reduction of eosin concentration of 50% and a reduction in eosin exposure time from 60 seconds to 5 seconds achieved similar eosin intensity between PFPE and FFPE sections. Hematoxylin

concentration and exposure time was not decreased in the current study, but one of the pathologists noted excess hematoxylin intensity and relative reduction of hematoxylin concentration or exposure time for PFPE sections should be considered in future studies.

The IHC comparison results are consistent with previously reported findings that staining PFPE tissue using IHC protocols developed with FFPE tissue often, but do not always give similar results. Further research is needed to determine which IHC protocols require adjustment for routine diagnostic use in PFPE tissue.

In summary, we found that preservation of prostate histomorphology in hematoxylin and eosin (H&E) stained PFPE tissue is comparable to that of FFPE and appears sufficient to support routine diagnostic surgical pathology. IHC-based detection of prostate cancer markers PSA, p63 + Ck5/6 and ERG is possible in PFPE prostate tissue without modification of protocols optimized for FFPE tissue. RNA and DNA isolated from PFPE tissue is substantially more intact compared to FFPE, RNA yield is greater from PFPE than FFPE tissue, and PFPE DNA and RNA is amenable to next generation sequencing (NGS) based methods of analysis. We propose the use of per-nucleus yields of DNA and RNA as benchmarks for future studies aiming to advance the basic science of tissue DNA and RNA preservation, extraction and analysis.

ACKNOWLEDGMENTS

The authors thank Marja Pirinen, Katja Liljeström, Marika Vähä-Jaakkola, Riina Kylätie, Päivi Martikainen, Anni Mäkinen, Toni Vormisto, Jan Silander, Tapio Lahtinen, and Mira Valkonen for excellent technical support, and thank Daniel Groelz (Qiagen) for discussions of results of Phase 1 of the study. Neither Qiagen nor any other reagent provider sanctioned or provided financial support for the study.

REFERENCES

1. Gillard M, Tom WR, Antic T, et al. Next-gen tissue: preservation of molecular and morphological fidelity in prostate tissue. *Am. J. Transl. Res.* 2015;7:1227.

2. Gündisch S, Slotta-Huspenina J, Verderio P, et al. Evaluation of colon cancer histomorphology: a comparison between formalin and PAXgene tissue fixation by an international ring trial. *Virchows Arch.* 2014;465:509–519. doi:10.1007/s00428-014-1624-4.

3. Mathieson W, Marcon N, Antunes L, et al. A Critical Evaluation of the PAXgene Tissue Fixation System: Morphology, Immunohistochemistry, Molecular Biology, and Proteomics. *Am. J. Clin. Pathol.* 2016;146:25–40. doi:10.1093/ajcp/aqw023.

4. Staff S, Kujala P, Karhu R, et al. Preservation of nucleic acids and tissue morphology in paraffin-embedded clinical samples: comparison of five molecular fixatives. *J. Clin. Pathol.* 2013;66:807–810. doi:10.1136/jclinpath-2012-201283.

5. Belloni B, Lambertini C, Nuciforo P, et al. Will PAXgene substitute formalin? A morphological and molecular comparative study using a new fixative system. *J. Clin. Pathol.* 2013;66:124–135. doi:10.1136/jclinpath-2012-200983.

6. Kap M, Smedts F, Oosterhuis W, et al. Histological Assessment of PAXgene Tissue Fixation and Stabilization Reagents. Moura IC, ed. *PLoS ONE* 2011;6:e27704. doi:10.1371/journal.pone.0027704.

7. Illumina technical note: Evaluating RNA Quality from FFPE Samples. Available at: https://www.illumina.com/content/dam/illumina-marketing/documents/products/technotes/evaluating-rna-quality-from-ffpe-samples-technical-note-470-2014-001.pdf. Accessed June 12, 2017

8. Advanced Analytical Technologies document: RNA_fragment-analyzer-correlation-legacy-data. Available at: https://www.aati-us.com/documents/brochures/rna_fragment-analyzer-correlation-legacy-data.pdf. Accessed June 12, 2017

9. Fawcett T. An introduction to ROC analysis. *Pattern Recognit. Lett.* 2006;27:861–874. doi:10.1016/j.patrec.2005.10.010.

10. Kim D, Pertea G, Trapnell C, et al. TopHat2: accurate alignment of transcriptomes in the presence of insertions, deletions and gene fusions. *Genome Biol.* 2013;14:R36. doi:10.1186/gb-2013-14-4-r36.

11. Quinlan AR, Hall IM. BEDTools: a flexible suite of utilities for comparing genomic features. *Bioinformatics* 2010;26:841–842. doi:10.1093/bioinformatics/btq033.

12. Langmead B, Salzberg SL. Fast gapped-read alignment with Bowtie 2. *Nat. Methods* 2012;9:357–359. doi:10.1038/nmeth.1923.

13. Faust GG, Hall IM. SAMBLASTER: fast duplicate marking and structural variant read extraction. *Bioinformatics* 2014;30:2503–2505. doi:10.1093/bioinformatics/btu314.

14. Li H, Handsaker B, Wysoker A, et al. The Sequence Alignment/Map format and SAMtools. *Bioinformatics* 2009;25:2078–2079. doi:10.1093/bioinformatics/btp352.

15. C-value [Wikipedia Web site]. 29 April 2017. Available at: https://en.wikipedia.org/wiki/C-value. Accessed June 12, 2017

16. Mizumachi T, Muskhelishvili L, Naito A, et al. Increased distributional variance of mitochondrial DNA content associated with prostate cancer cells as compared with normal prostate cells. *The Prostate* 2008;68:408–417. doi:10.1002/pros.20697.

17. Reznik E, Miller ML, Şenbabaoğlu Y, et al. Mitochondrial DNA copy number variation across human cancers. *eLife* 2016;5. doi:10.7554/eLife.10769.

18. Do H, Dobrovic A. Sequence Artifacts in DNA from Formalin-Fixed Tissues: Causes and Strategies for Minimization. *Clin. Chem.* 2015;61:64–71. doi:10.1373/clinchem.2014.223040.

19. Costello M, Pugh TJ, Fennell TJ, et al. Discovery and characterization of artifactual mutations in deep coverage targeted capture sequencing data due to oxidative DNA damage during sample preparation. *Nucleic Acids Res.* 2013;41:e67–e67. doi:10.1093/nar/gks1443.

20. Kim S, Park C, Ji Y, et al. Deamination Effects in Formalin-Fixed, Paraffin-Embedded Tissue Samples in the Era of Precision Medicine. *J. Mol. Diagn.* 2017;19:137–146. doi:10.1016/j.jmoldx.2016.09.006.

21. Carrick DM, Mehaffey MG, Sachs MC, et al. Robustness of Next Generation Sequencing on Older Formalin-Fixed Paraffin-Embedded Tissue. Zuo Z, ed. *PLOS ONE* 2015;10:e0127353. doi:10.1371/journal.pone.0127353.

22. Greagg MA, Fogg MJ, Panayotou G, et al. A read-ahead function in archaeal DNA polymerases detects promutagenic template-strand uracil. *Proc. Natl. Acad. Sci.* 1999;96:9045–9050. doi:10.1073/pnas.96.16.9045.

23. Herculase II Fusion DNA Polymerase User Manual. Available at: http://www.agilent.com/cs/library/usermanuals/Public/600675.pdf. Accessed June 12, 2017

FIGURE LEGENDS

FIGURE 1. Study design. Overview of the methods used in the 4-core study (A) and subsequent 3-core study (B). Results from both phases of the study are reported, with emphasis on the 3-core study, where improved RNA quality was obtained. FF: Fresh frozen; FFPE: Formalin-fixed paraffin embedded; PFPE: PAXgene-fixed paraffin embedded.

FIGURE 2. Overview of core sectioning. Consecutive sections were cut from each of the cores for H&E, IHC and nucleic acid extraction as indicated in the figure and in Materials and Methods. FF: Fresh frozen; FFPE: Formalin-fixed paraffin embedded; PFPE: PAXgene-fixed paraffin embedded.

FIGURE 3. Representative histomorphology of formalin-fixed paraffin-embedded (FFPE) and Paxgene-fixed paraffin-embedded (PFPE) tissue containing cancer. Representative examples of H&E (left) and 2IHC (CK5/6, p63 and AMACR, right) stained FFPE (A, B) or PFPE (C, D) cores from case PAX 89. 100 micron width reference bar shown. See Supplemental Figure 3 for a second set of representative images from PAX 69.

FIGURE 4. Genomic DNA yield and quality. A) Genomic Quality Number GQN measured with Fragment Analyzer are shown for A, B and C cores in the 16 cases in the 3-core study. B, Fragment Analyzer DNA tracings from representative samples from A (blue), B (red) and C (green) cores (RFU, Relative Fluorescence Units). C, qPCR-based quality control (FFPE QC Kit, Illumina) ΔCt values (Core DNA Ct-QC kit template DNA Ct) for amplified DNA. A ΔCt value of ≤ 2 is considered good quality DNA. D, Estimated picogram DNA yield per nucleus based on nucleus counts performed as described in Materials and Methods. Mean and SD shown for each group (n=16), ** $p<0.01$, *** $p<0.001$. FF: Fresh frozen; FFPE: Formalin-fixed paraffin embedded; PFPE: PAXgene-fixed paraffin embedded. GQN values in the 20-case 4-core study were similar.

FIGURE 5. Total RNA yield and quality. A, RNA Quality Number (RQN) measured with Fragment Analyzer are shown for A, B and C cores in the 16 cases in the 3-core study. B, Fragment Analyzer RNA tracings from representative samples from A (blue), B (red) and C (green) cores. C, RNA sequencing of RNA isolated from A, B and C core tissue from four

representative cases (PAX 84, 85, 91 and 96). Boxplot displaying the distributions of coverage at each position of 22 target transcripts in MiSeq (Illumina) RNA. The values are log2-transformed for better visualization. The boxes span the interquartile range (IQR) of the values, with the lines inside the boxes showing the medians, and whiskers above and below the boxes showing the locations of the minimum and maximum data points within 1.5 times the IQR. D, Estimated picogram RNA yield per nucleus. Mean and SD are shown for each group (n=16).* $p<0.05$, ** $p<0.01$, *** $p<0.001$. FF: Fresh frozen; FFPE: Formalin-fixed paraffin embedded; PFPE: PAXgene-fixed paraffin embedded.

TABLES

Table 1. Key tissue collection time, weight, and temperature data means (standard deviations) from the 4-core and 3-core studies.

Phase of Study	Time between leaving body and arriving in pathology (h:mm)	Prostate weight (grams)	Prostate core temperature on arrival in pathology laboratory (Celsius)	Prostate core temperature low point after cooling (Celsius)	Total cooling time (h:mm)	Total time from removal from body to time in fixative (h:mm)	Total time from patient start anesthesia to time in fixative (h:mm)	Total time from first artery ligation to time in fixative (h:mm)	Total operating time from first trocar to time prostate out of body (h:mm)
4-core (initial phase, 20 cases over 6 weeks in 2015	0:15 (0:13)	56.7 (16.6)	27.7 (3)	13.8 (2.3)	0:11 (0:06)	0:52 (0:13)	3:35 (0:57)	1:44 (0:29)	2:21 (0:49)
3-core (second phase, 16 cases over 2 weeks in 2015	0:14 (0:11)	54.2 (17)	27.6 (2.1)	14.6 (0.9)	0:07 (0:03)	0:40 (0:13)	2:52 (0:46)	1:23 (0:20)	1:55 (0:40)
p-value	n.s.	n.s.	n.s.	n.s.	$p<0.05$	$p<0.05$	$p<0.05$	$p<0.05$	n.s.

Table 2. Summary of genomic DNA and total RNA quality for A, B and C core groups in the 3-core study.

Core group	Fixation method	Extraction method (Qiagen)	DNA yield (ng)/ 6.2 mm^3	DNA GQN	Average DNA fragment length (bp)	RNA yield (ng)/6.2 mm^3	RNA RQN	RNA DV_{200}
A	Fresh Frozen (FF)	Allprep Universal	1261 ± 470	7.9 + 0.4	58939 ± 2989	4341 ± 1683	8.7 ± 0.9	80.8 ±3.8
B	Formalin-fixed paraffin embedded (FFPE)	Allprep FFPE	2786 ±1383	3.2 + 0.5	19680 ± 2418	3726 ± 2242	2.6 ± 1.2	49.8 ±13.4
C	PAXgene-fixed paraffin embedded (PFPE)	Paxgene Allprep	2718 ± 1562	6.2 + 0.9	41274 ± 9216	7806 ± 2970	6.3 ± 0.3	75.5 ±3.4

GQN: Genomic Quality Number; RQN: RNA Quality Number; DV_{200}: percentage of RNA over 200 nucleotides in size

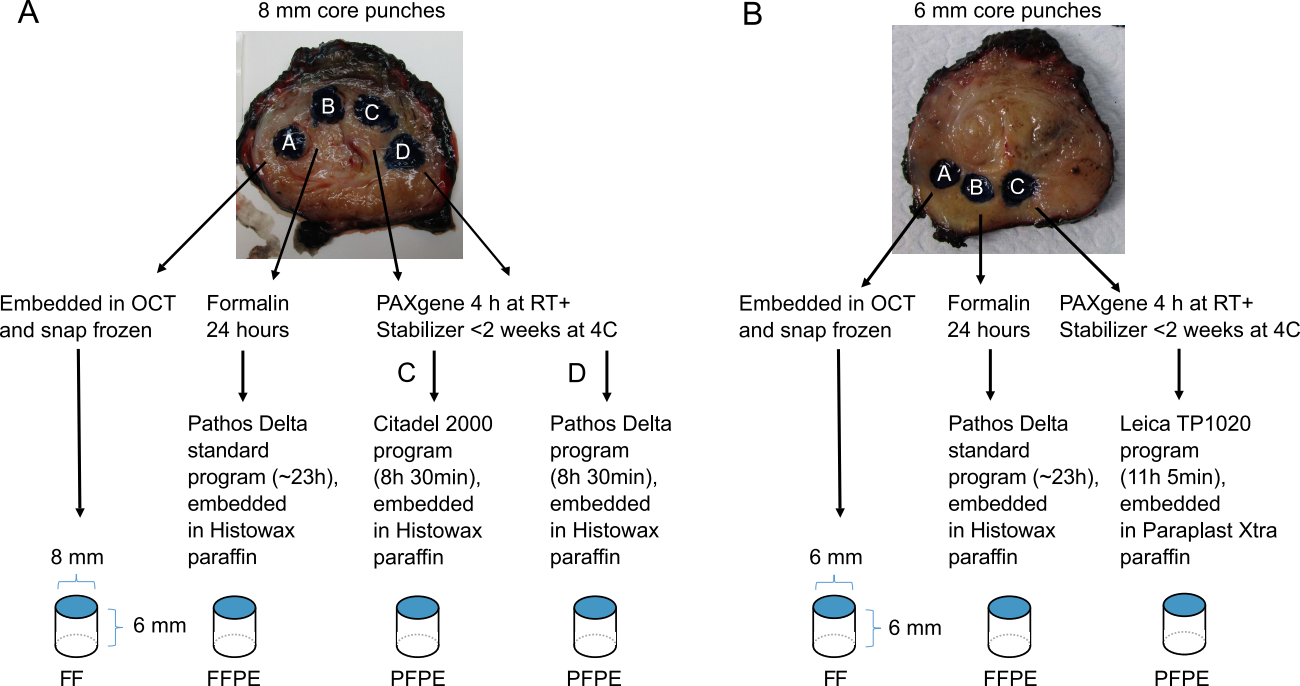
A
8 mm core punches
B
C
A
D
Embedded in OCT and snap frozen
Formalin 24 hours
PAXgene 4 h at RT+ Stabilizer <2 weeks at 4C
C
D
Pathos Delta standard program (~23h), embedded in Histowax paraffin
Citadel 2000 program (8h 30min), embedded in Histowax paraffin
Pathos Delta program (8h 30min), embedded in Histowax paraffin
8 mm
6 mm
FF
FFPE
PFPE
PFPE
B
6 mm core punches
A
B
C
Embedded in OCT and snap frozen
Formalin 24 hours
PAXgene 4 h at RT+ Stabilizer <2 weeks at 4C
Pathos Delta standard program (~23h), embedded in Histowax paraffin
Leica TP1020 program (11h 5min), embedded in Paraplast Xtra paraffin
6 mm
6 mm
FF
FFPE
PFPE

FF (A) cores

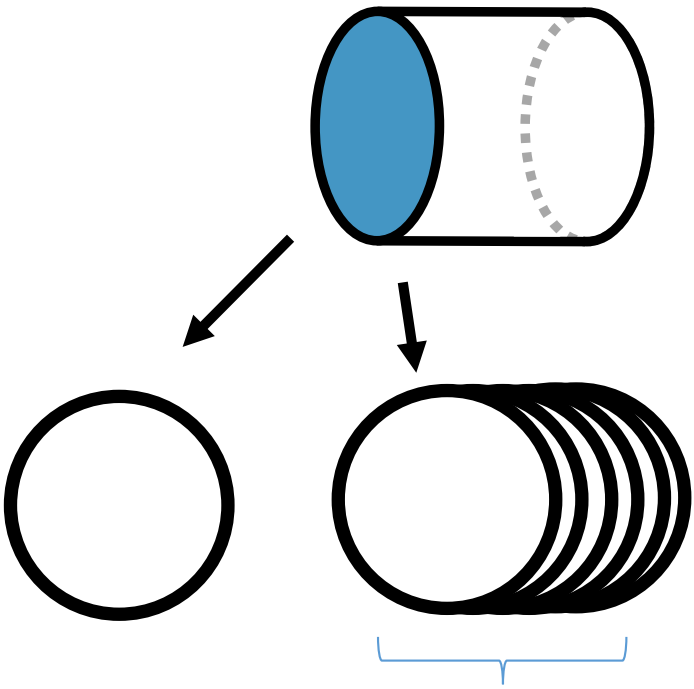

H&E

12 or 22x10 µm
DNA/RNA

FFPE (B) & PFPE (C&D) cores

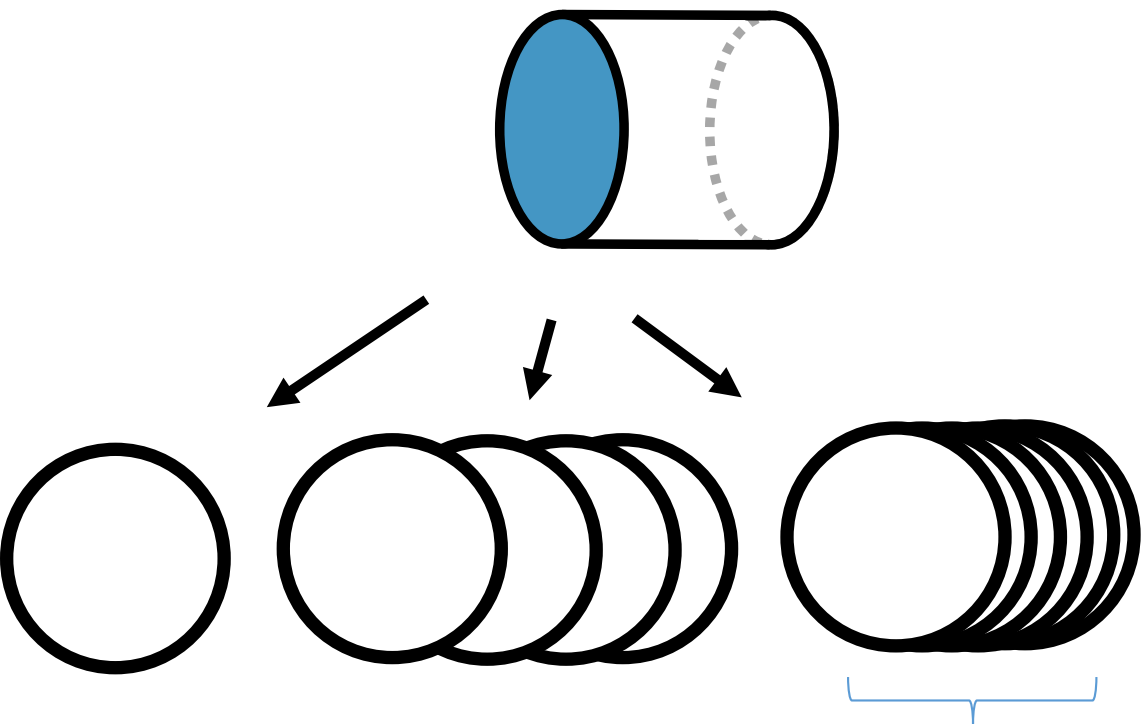

H&E

IHC: PSA, ERG,
VIM & 2IHC

12 or 22x10 µm
DNA/RNA

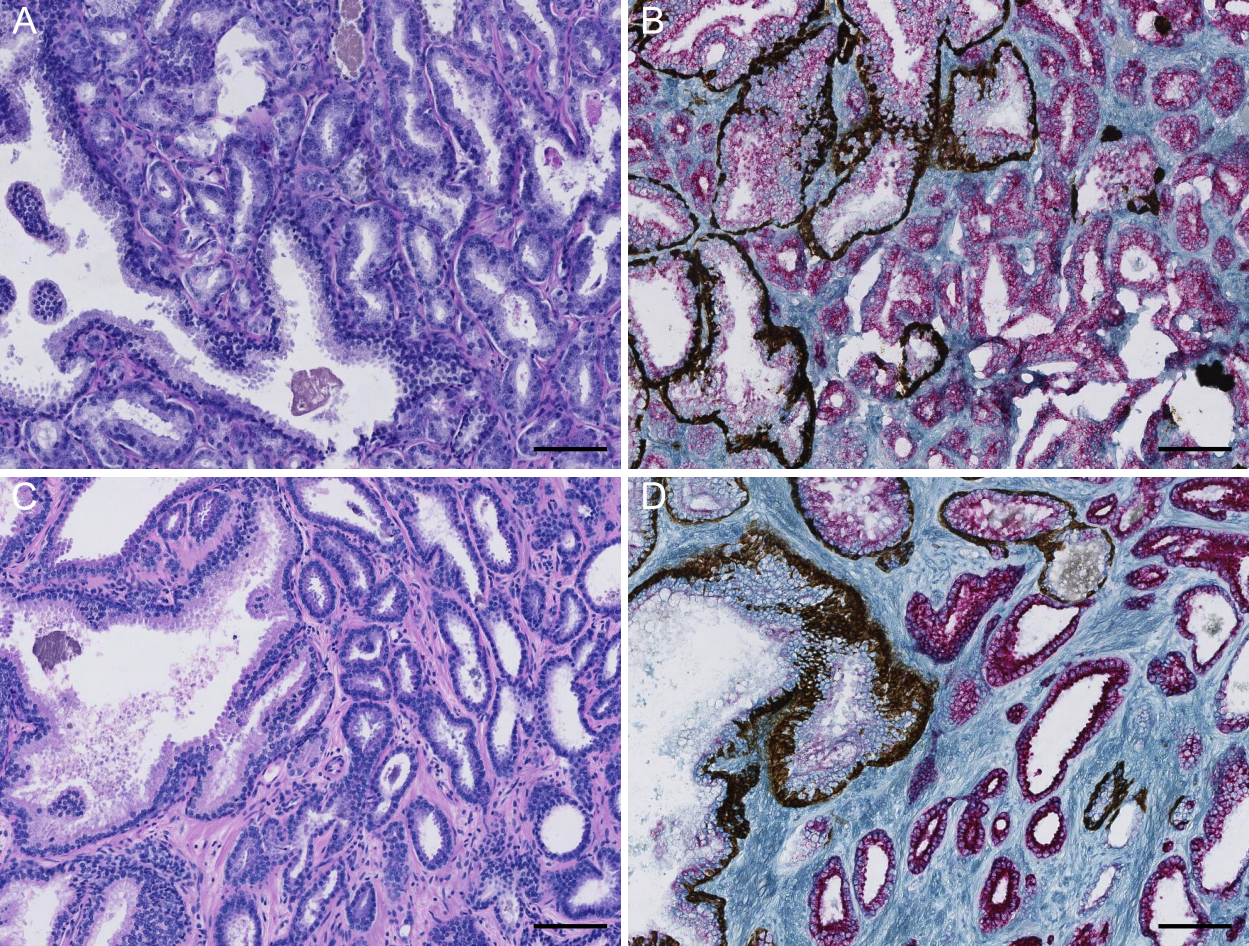
A
B
C
D

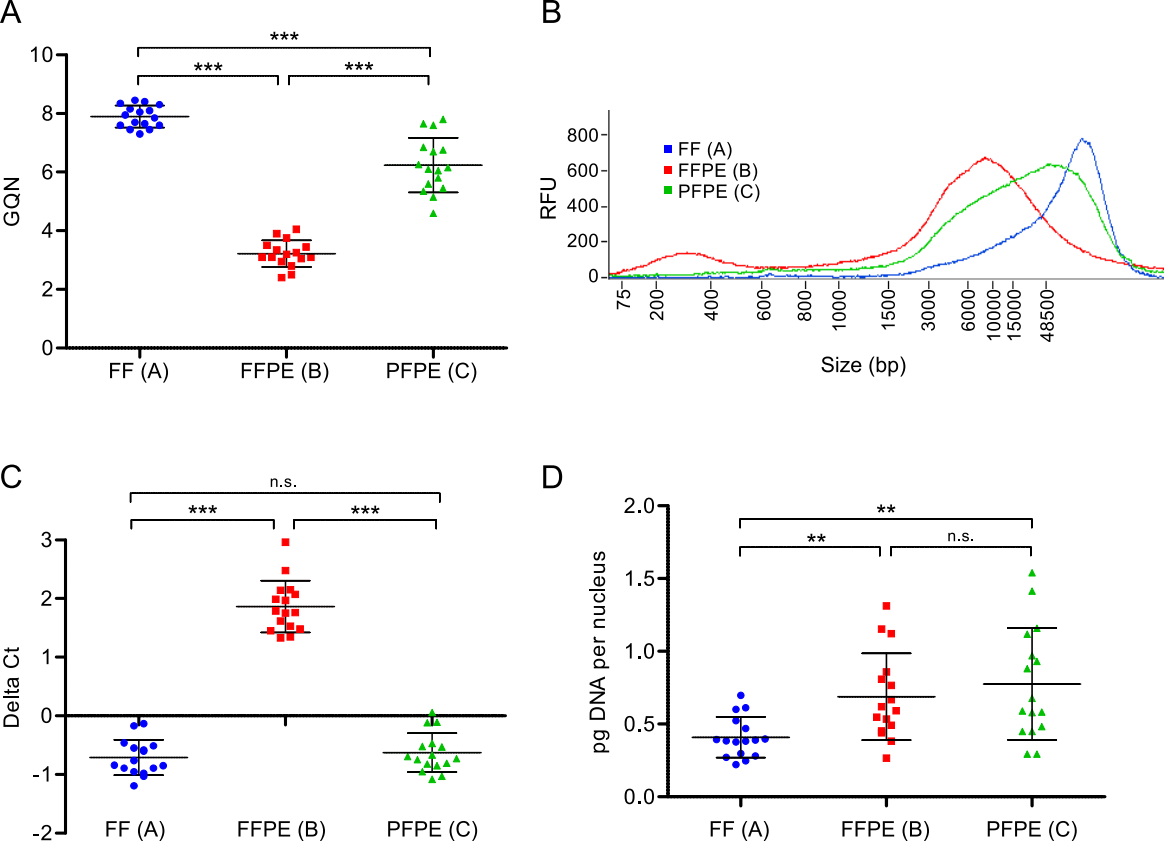
A
***
***
***
GQN
10
8
6
4
2
0
FF (A)
FFPE (B)
PFPE (C)
B
RFU
800
600
400
200
0
FF (A)
FFPE (B)
PFPE (C)
75
200
400
600
800
1000
1500
3000
6000
10000
15000
48500
Size (bp)
C
n.s.
***
***
Delta Ct
3
2
1
0
-1
-2
FF (A)
FFPE (B)
PFPE (C)
D
**
**
n.s.
pg DNA per nucleus
2.0
1.5
1.0
0.5
0.0
FF (A)
FFPE (B)
PFPE (C)

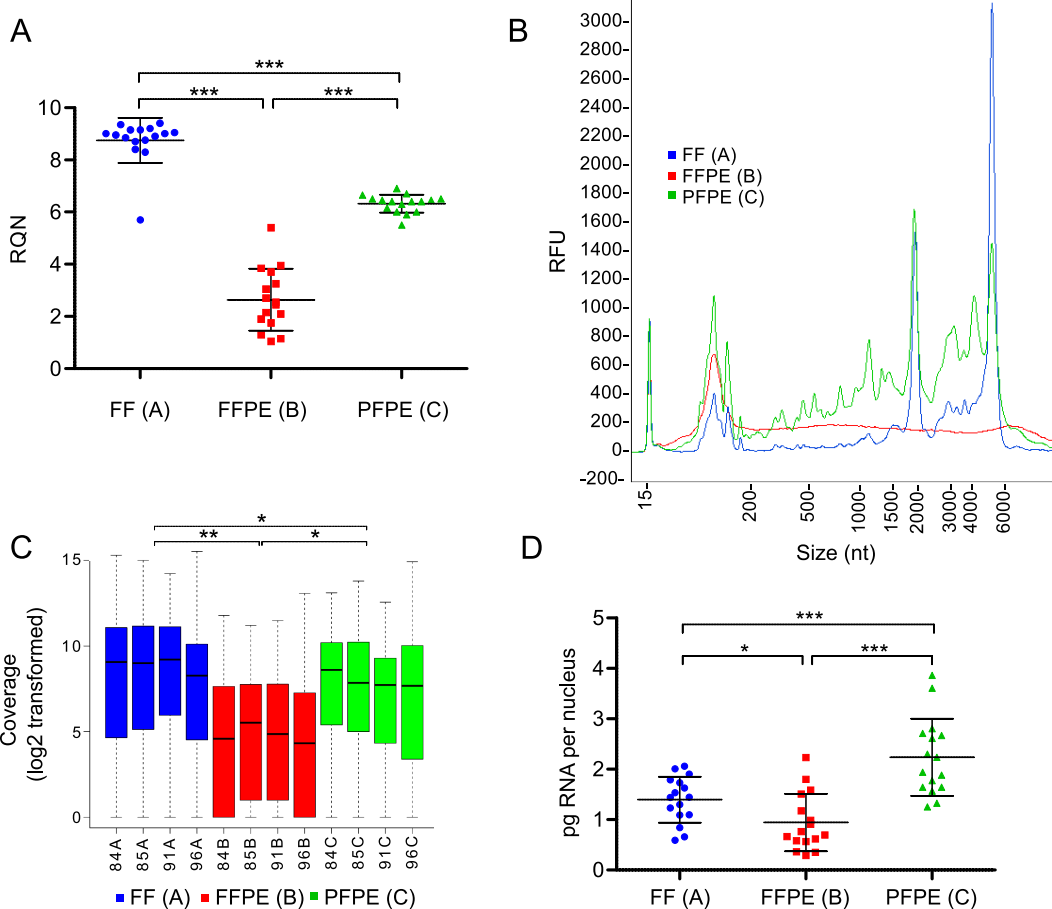
A
***
***
***
RQN
10
8
6
4
2
0
FF (A)
FFPE (B)
PFPE (C)
B
RFU
3000
2800
2600
2400
2200
2000
1800
1600
1400
1200
1000
800
600
400
200
0
-200
FF (A)
FFPE (B)
PFPE (C)
15
200
500
1000
1500
2000
3000
4000
6000
Size (nt)
C
*
**
*
Coverage
(log2 transformed)
15
10
5
0
84A
85A
91A
96A
84B
85B
91B
96B
84C
85C
91C
96C
FF (A)
FFPE (B)
PFPE (C)
D
***
*
***
pg RNA per nucleus
5
4
3
2
1
0
FF (A)
FFPE (B)
PFPE (C)

Supplemental Digital Content

Feasibility of prostate PAXgene fixation for molecular research and diagnostic surgical pathology: Comparison of matched fresh frozen, FFPE and PFPE tissues.

Gunilla Högnäs, PhD,* Kati Kivinummi, PhD,* Heini M.L. Kallio PhD,* Reija Hieta, PhD,* Pekka Ruusuvuori, DSc,*□ Antti Koskenalho MS,* Juha Kesseli PhD,* Teuvo L.J. Tammela MD PhD,*† Jarno Riikonen MD PhD,† Joanna Ilvesaro, PhD,¶ Saara Kares,¶ Pasi P. Hirvikoski, MD PhD,# Marita Laurila, MD,¶ Tuomas Mirtti MD PhD,‡ Matti Nykter PhD,* Paula M. Kujala, MD,¶ Tapio Visakorpi, MD PhD,*¶ Teemu Tolonen, MD PhD,¶ and G. Steven Bova, MD,*

*Prostate Cancer Research Center, Faculty of Medicine and Life Sciences and BioMediTech Institute, University of Tampere, Tampere, FI-33014, Finland

□Tampere University of Technology, Pori, Finland.

†Department of Urology, University of Tampere, Tampere University Hospital, Tampere, Finland

¶Department of Pathology, Tampere University Hospital, Fimlab Laboratories, Tampere, Finland

#Department of Pathology, Oulu University Hospital, Oulu, Finland

‡Institute for Molecular Medicine Finland, University of Helsinki, Helsinki, Finland; Department of Pathology, HUSLAB, Helsinki University Hospital, Helsinki, Finland.

Correspondence to: G. S. Bova, University of Tampere, BioMediTech, P.O. Box 100, FI-33014 Tampere, Finland; g.steven.bova@uta.fi

CONTENTS

SUPPLEMENTAL METHODS 3
SUPPLEMENTAL FIGURES 5
Supplemental Figure 1. 3- and 4-core study PFPE RNA quality 5
Supplemental Figure 2. Red blood cell morphology 6
Supplemental Figure 3. Histomorphology of formalin-fixed paraffin-embedded (FFPE) and Paxgene-fixed paraffin-embedded (PFPE) tissue containing cancer 6
Supplemental Figure 4. Genomic DNA agarose gel electrophoresis 7
Supplemental Figure 5. Genomic DNA yield and quality 8
Supplemental Figure 6. Nucleic acid quality and yield 9
SUPPLEMENTAL TABLES 10
Supplemental Table 1. Summary of 4-core and 3-core methods and results 10
Supplemental Table 2. Pathos DELTA tissue processing protocol for formalin-fixed B cores in the 3-core and 4-core studies. 11
Supplemental Table 3. Citadel 2000 (69810051 Issue 18) tissue processing protocol for PAXgene-fixed C cores in the 4-core study. 12
Supplemental Table 4. Pathos DELTA tissue processing protocol for PAXgene-fixed D cores in the 4-core study. 12
Supplemental Table 5. Leica TP1020 tissue processing protocol for PAXgene-fixed C cores in the 3-core study. 12
Supplemental Table 6. BioMediTech H&E staining protocol for FFPE B and donor macro sections, and PFPE C and D cores in 4-core study 13
Supplemental Table 7. BioMediTech H&E staining protocol for FF A cores in 4-core study 13
Supplemental Table 8. Fimlab pathology laboratory H&E staining protocol for FFPE B cores in 3-core study 14
Supplemental Table 9. BioMediTech H&E staining protocol for PFPE C cores in 3-core study 14
Supplemental Table 10. BioMediTech H&E staining protocol for FF A cores in 3-core study 15
Supplemental Table 11. DNA MiSeq assay target list 15
Supplemental Table 12. RNA MiSeq assay Target List 16
Supplemental Table 13. Summary of nucleus counts in the 3-core study 16

SUPPLEMENTAL METHODS

Processing Chemicals

Chemicals used in tissue processing and staining listed in the tables below used in the 4-core study Pathos DELTA and Citadel processors were the same products from the same manufacturers but not the same lot numbers due to different ordering logistics in each location. Processing and staining chemicals used in the 3-core study Pathos DELTA and Leica TP1020 processors were from the same manufacturers and lot numbers.

Standard Fimlab Prostate External Inking for Surgical Margin Analysis

Using correct inking technique (complete coverage using cotton applicator (Ref 120783, Selefa OneMed) then dried with paper towels) black ink (CAT# WAK-HM-B-3, WAK-Chemie Medical GmbH) was placed on the surface of the left side and on the whole posterior surface, blue ink (CAT# WAK-HM-BL-5, WAK-Chemie Medical GmbH) on the surface of the right side and green ink (CAT# WAK-HM-G-1, WAK-Chemie Medical GmbH) on the anterior apex and anterior base. Inking was performed with "clean" technique, wearing non-sterile gloves, non-sterile cotton applicators, and non-sterile ink as supplied by the manufacturer.

Web-Based Blinded, Randomized Survey of FFPE vs PAXgene fixed tissue histology

All cores containing cancer from the 3-core and 4-core study were included in the survey. Cores containing no cancer were excluded since adenocarcinoma is the main focus of surgical pathology evaluation of radical prostatectomy specimens. Provided onscreen to each pathologist with the survey:

Title of Survey: Surgical Pathology Adequacy Survey
Instructions: 8mm and 6mm punches taken from 6mm thick radical prostatectomy transverse sections were fixed in either PAXgene or Formalin using standard procedures, and sections were cut for H&E and 2IHC (AMACR, p63 and cytokeratin 5/6) staining. With each question you will be presented with the H&E and 2IHC stain from the same core. The images of the H&E and 2IHC sections are from the same block but may not be in the same orientation. Questions refer to each HE/2IHC pair.

Questions with each zoomable image pair from the same tissue block, with no identifier provided (H&E on left, 2IHC stain on right):
1 - What is your best estimate of how the source tissue block was prepared? (required dropdown selection: Formalin-Fixed Paraffin-Embedded or PAXgene-fixed Paraffin-Embedded)
2 - What visual clues are you using to identify the tissue as processed in this way? (optional free text field)

3 - Taking into account the H&E and 2IHC staining, does the quality appear adequate for routine radical prostatectomy surgical pathology analysis, such as identification of cancer cells, and Gleason scoring? (required dropdown selection: yes/no)
4 - Please state what is not adequate (optional free text field)

Qiagen Kit Extraction modifications

Isolation of 3-core study FFPE (B Core) and 4-core study FFPE (B core) and PFPE (C and D core RNA and DNA was done using Qiagen's Allprep DNA/RNA FFPE kit (cat no 80234) or the PAXgene Tissue Allprep DNA/RNA/miRNA method (Qiagen's PX10 Supplemental protocol) according to manufacturer's instructions, apart from the deparaffinization steps. 1400 µl heptane was added to the cut paraffin sections, the tubes were vortexed vigorously for 10s and incubated 20 min at 37°C. 70 µl methanol was added, the samples vortexed and centrifuged for 2 min at 9000 x g. The supernatant was carefully removed using a pipet, 1.4 ml ethanol added to the pellet followed by vortexing and centrifugation for 2 min at full speed. The supernatant was removed and the ethanol wash repeated.

3-core PFPE (C core) DNA and RNA were isolated with the PAXgene Tissue Allprep DNA/RNA/miRNA method (PX10 supplementary protocol) according to manufacturer's instructions, apart from a small modification in the deparaffinization step. 650 ul xylene was added to cut paraffin sections, the tubes were vortexed vigorously for 20s and incubated 10 min on the benchtop before continuing with ethanol washing according to protocol.

Immunohistochemistry staining protocols:

All immuno stains (2IHC, PSA, ERG and Vimentin) were done at Fimlab according to their standard staining protocols for their own diagnostic purposes and counterstained with hematoxylin.

PSA-stain:

- Automated Bond III technology
- Leica Bond™ Polymer Refine Detection-kit
- Pretreated 30min with Bond Epitope Retrieval Solution 1
- Hybridized with Dako (A0562 Clone, 1:15000 dilution) against PSA

ERG-stain:

- Automated Bond III technology
- Leica Bond™ Polymer Refine Detection-kit
- Pretreated 30min with Bond Epitope Retrieval Solution 2
- Hybridized with Biocare Medical antibody (CM421C Clone: 9FY, 1:500) against ERG.

LeicaVimentin-stain:

- Automated Bond III technology
- Leica Bond™ Polymer Refine Detection-kit
- Pretreated 20min with Bond Epitope Retrieval Solution 1
- Hybridized with Leica RTU PA0033 (Clone: SRL33) against Vimentin.

2IHC-stain (AMACR, p63 and cytokeratin 5/6):

- Automated Ventana Benchmark GX technology
- Optiview-kit (brown for p63 and KRT5/6) and Ultraview Alkaline Phosphatase Red (for AMACR)
- AMACR-anitibody: Sigma Aldrich HPA019527-100UL (Polyclonal, 1:2000)
- p63-antibody: Bio SB (BSB5853, Clone: 4A4, 1:100)
- cytokeratin 5/6 antibody: Zymed 18-0267 (Clone: D5/16 B4, 1:100)

SUPPLEMENTAL FIGURES

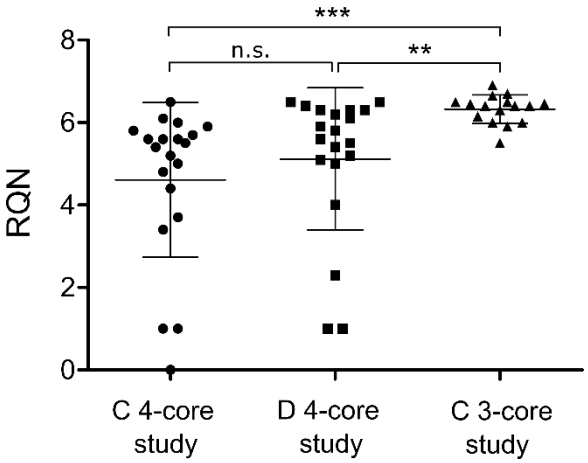

Supplemental Figure 1. 3- and 4-core study PFPE RNA quality. Mean and SD are shown, n=16 for 3-core and n=20 for 4-core study samples. **p<0.01,*** p<0.001.

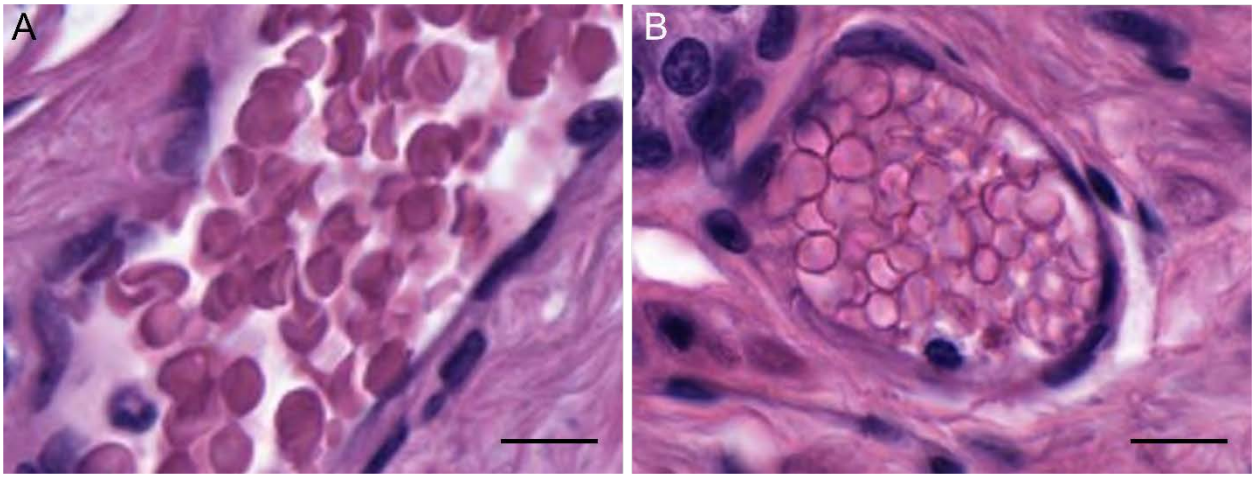

Supplemental Figure 2. Red blood cell morphology. Representative examples of H&E stained red blood cells from FFPE (A) and PFPE (B) cores from case PAX69. 10 micron width reference bar shown.

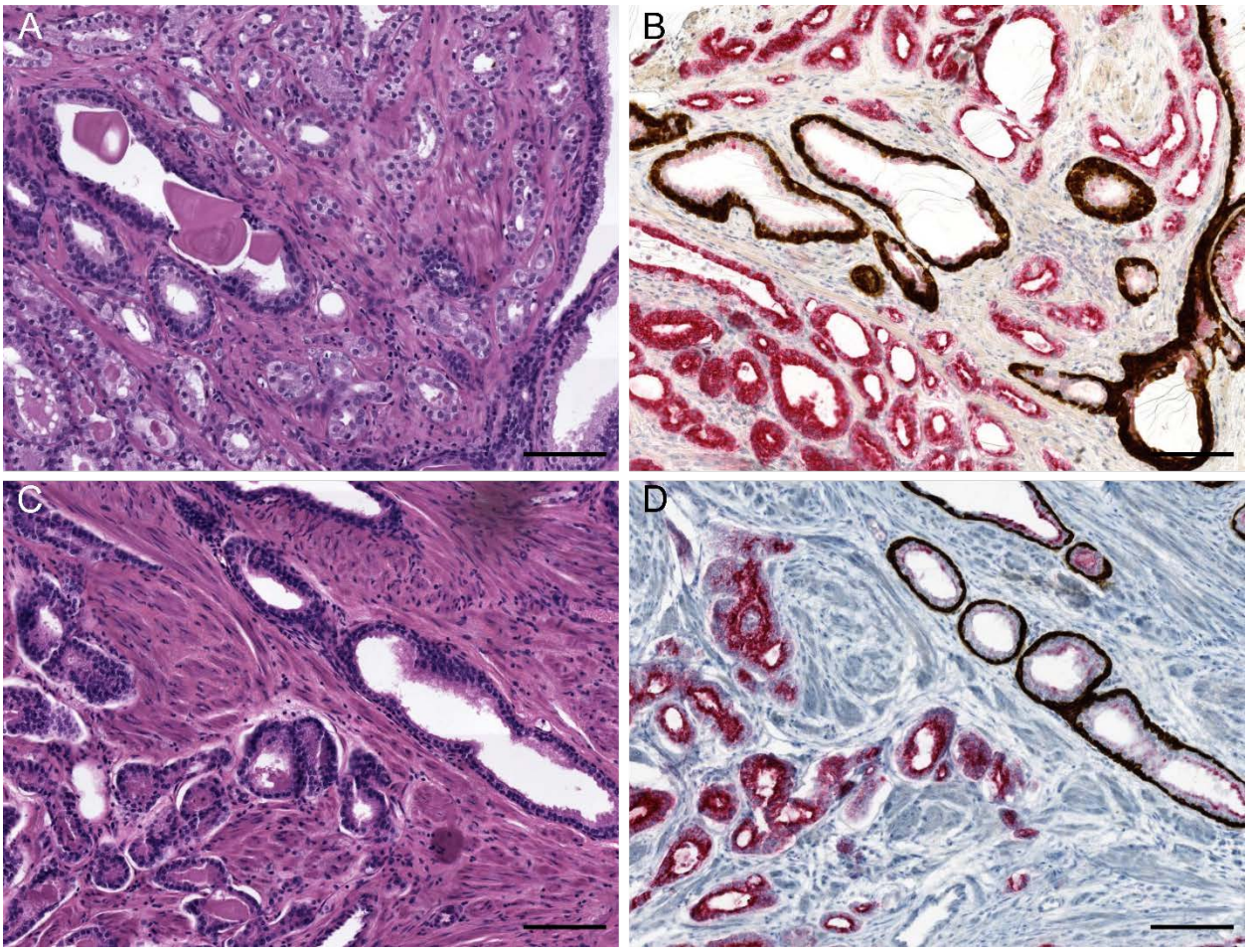

Supplemental Figure 3. Histomorphology of formalin-fixed paraffin-embedded (FFPE) and Paxgene-fixed paraffin-embedded (PFPE) tissue containing cancer. Representative examples of H&E (left) and 2IHC (CK5/6, p63 and AMACR, right) stained FFPE (A, B) or PFPE (C, D) sections from case PAX 69. 100 micron width reference bar shown.

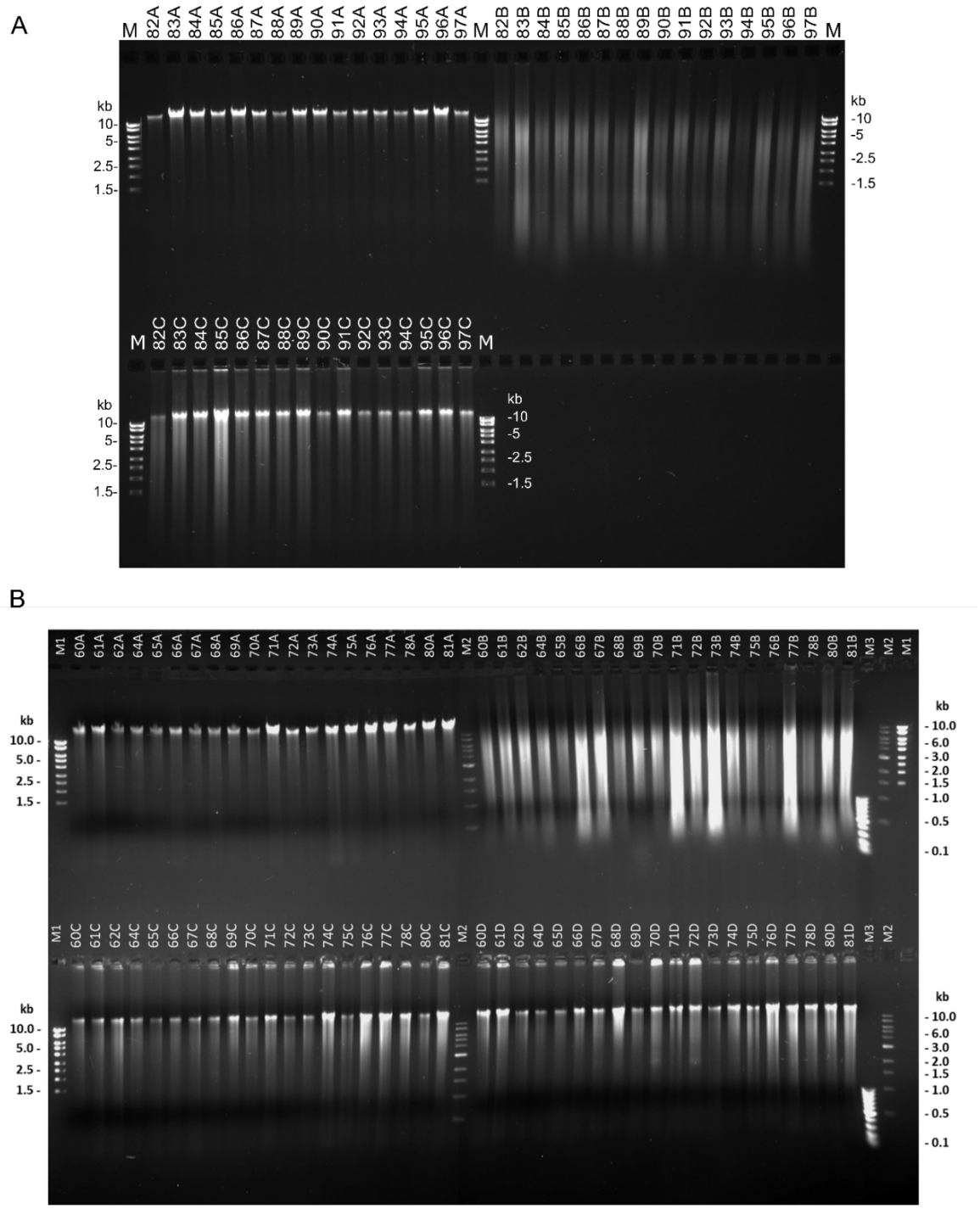

Supplemental Figure 4. Genomic DNA agarose gel electrophoresis. A, 3.0 µL of each undiluted, original 3-core study DNA sample (PAX 82-97 A, B and C cores) were loaded with 6x DNA loading buffer into a 0.6% agarose gel with 0.5x SYBR Safe DNA dye (Thermo Scientific). Electrophoresis was performed in 0.5 X TBE buffer at 80 V for 70 min, after which the gel was visualized under UV-light (800 ms). The sample labels for all PAX cores are shown above each well and DNA size markers are illustrated on the left and right sides of the figure. 2 µL of MassRuler™ High Range DNA Ladder (Thermo Scientific) is used as marker. B, 3.0 µL of each undiluted, original 4-core study DNA sample was loaded with DNA loading buffer into 0.6% Agarose gel. Electrophoresis was performed in 0.5 X TE buffer, EtBr 165 µg/mL, at 120 V

for 50 min after which the gel was visualized under UV-light (720 ms). M1: 2 µL of MassRuler™ High Range DNA Ladder (Thermo Scientific), M2: 2 µL of 1 kb DNA Ladder (NEB), M3: 2 µL of GeneRuler™ 100 bp DNA Ladder (Thermo Scientific).

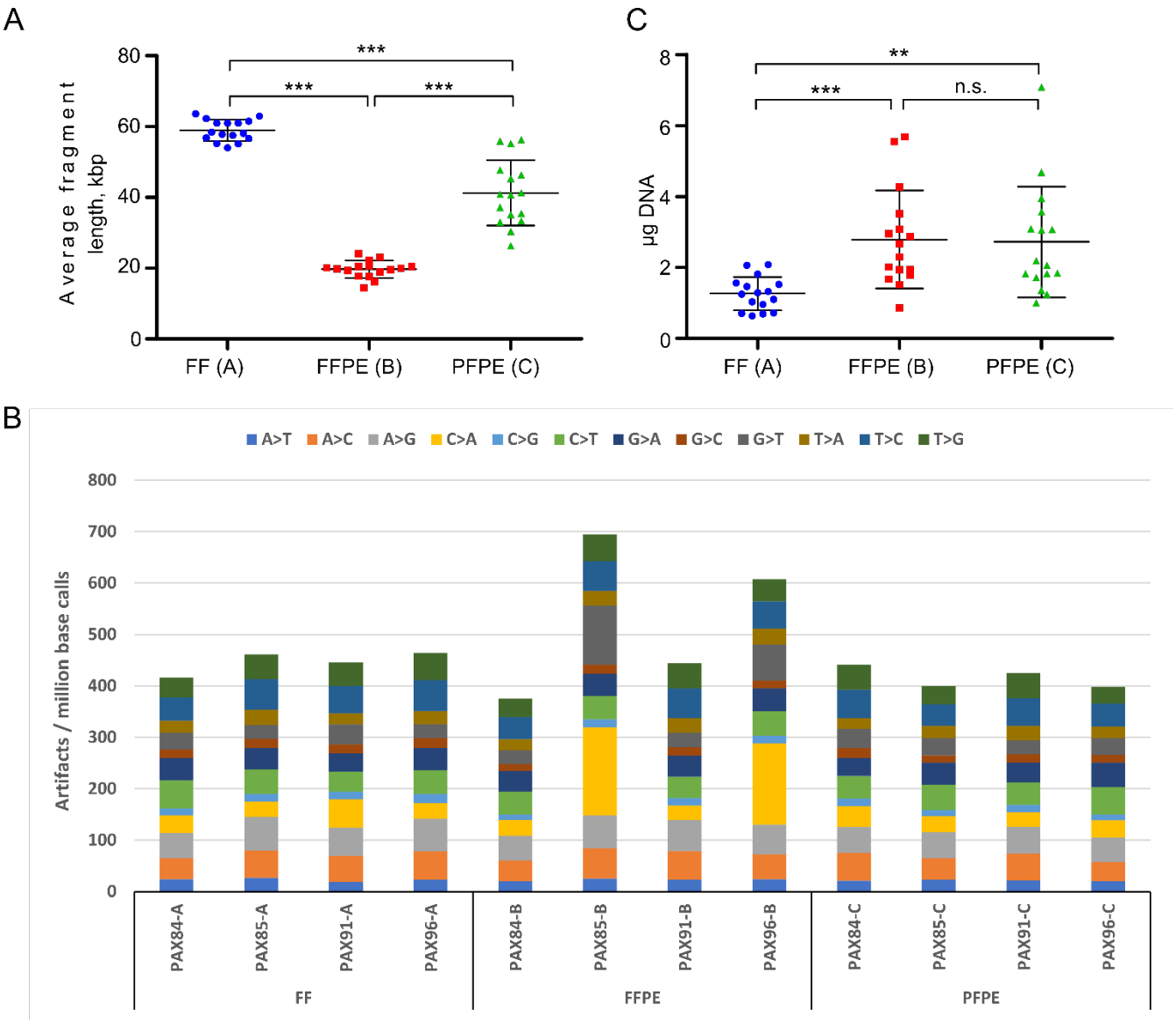

Supplemental Figure 5. Genomic DNA yield and quality. A, Average DNA fragment length (bp) of two Fragment Analyzer measurements is shown for each individual core sample for the A, B and C cores. B, Sequencing artefacts in DNA MiSeq. The bars show the frequencies of the indicated base changes per million corresponding correct base calls (the count of A>A, C>C, G>G, or T>T base calls) in the 1-10% variant allele frequency range. C, Genomic DNA yield per 6.2 mm^3 tissue volume measured with Qubit 2.0. Mean and SD are shown for each group (n=16). **p<0.01, *** p<0.001. FF: Fresh frozen; FFPE: Formalin-fixed paraffin embedded; PFPE: PAXgene-fixed paraffin embedded.

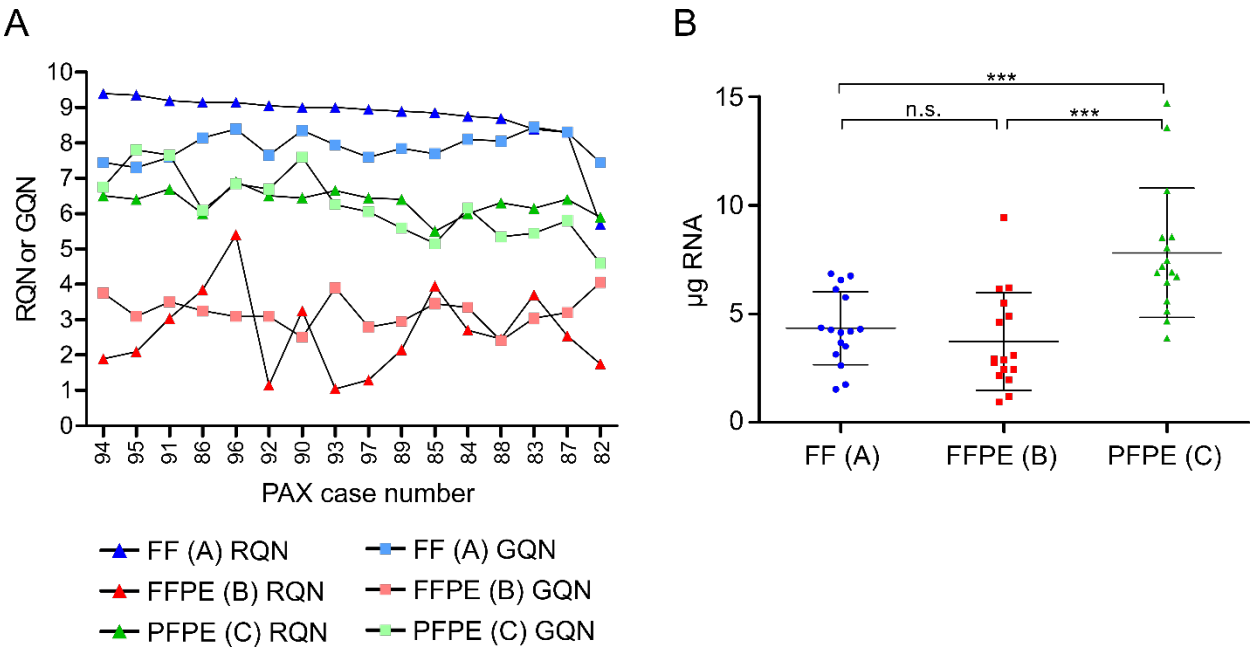

Supplemental Figure 6. Nucleic acid quality and yield. A, RQN and GQN values from matched A, B and C samples ordered in decreasing RQN values of A cores from the 3-core study. B, Total RNA yield per 6.2 mm^3 tissue volume measured with Fragment Analyzer. Mean and SD are shown for each group (n=16). *** $p<0.001$. FF: Fresh frozen; FFPE: Formalin-fixed paraffin embedded; PFPE: PAXgene-fixed paraffin embedded.

SUPPLEMENTAL TABLES

Supplemental Table 1. Summary of 4-core and 3-core methods and results.

	4-core study (first phase)	3-core study (final phase)
RALP Patient Cohort	20 men	16 men
Fixation method of whole mount donor tissue section	Tissue section placed between two pieces of nylon and polyester sheets inside a 200ml container, keeping the tissue flat during fixation.	Tissue section placed in a Supa Mega Slim white cassette (CellPath, EAN 0102-02A)
Core punches	4 cores, 8 mm diameter, taken as depicted in Fig. 1A	3 cores, 6 mm diameter taken as depicted in Fig. 1B. Coring was shifted to the posterior side to increase likelihood of having cancer in the core, since prostate cancer is more often found posteriorly. Core diameter was decreased since the 8 mm cores suggested smaller cores would provide sufficient area for histologic assessment while allowing the three cores to sample more closely related areas of each prostate.
Tissue processing	B cores: Fimlab pathology laboratory standard Pathos DELTA protocol for formalin tissue; C: Citadel 2000 processor, optimized for PAXgene tissue; D: Pathos DELTA processor, optimized for PAXgene tissue	B cores: Fimlab pathology laboratory standard Pathos DELTA protocol for formalin tissue ; C: Dedicated Leica TP1020 optimized for PAXgene tissue
Embedding Paraffin	B, C, and D cores: Histowax, Histolab	B cores: Histowax, C Cores: Paraplast Xtra, P3808 Sigma-Aldrich
Deparaffinization	B, C, and D cores: Heptane (see Supplemental Methods above)	B cores: Heptane, C cores: Xylene (see Supplemental methods above)
H&E staining	Standard staining protocol for FF sections (Supp Table 7). The same protocol for B, C and D cores (Supp Table 6).	C (Supp Table 9) and A core (Supp Table 10) protocols optimized to match Fimlab standard B core staining (Supp Table 8) protocol intensities.
Scanning	Olympus BX51 with Olympus UplanSApo 40x objective and Surveyor Software, Objective Imaging Ltd.	Hamamatsu Photonics Nano Zoomer XR C12000 automated scanner with 0.23µm/pixel resolution.
Anesthesia agents and other drugs during surgery	Cefuroxine 1,5 g, Propofol 2%, Remifentalil 50mg, Rocuron 30-50 mg	Cefuroxine 1,5 g, Propofol 2%, Remifentalil 50mg, Rocuron 30-50 mg
Surgical Pathology Report Gleason grades (# patients)	3+3 (2), 3+4 (11), 4+3 (5), 4+4 (1), 4+5 (1)	3+4 (9), 4+3 (4), 4+4 (1), 4+5 (1), 5+3 (1)
pTNM staging (# patients)	pT2a (1), pT2c (11), pT3a (7), pT3b (1)	pT2a (1), pT2b (3), pT2c (2), pT3a (7), pT3b (3)
DNA Quality	Average GQN: FF (A cores) 8.2, FFPE (B cores) 4.0 PFPE (C cores) 6.8 and PFPE (D cores) 7.0	Average GQN: FF (A cores) 7.9, FFPE (B cores) 3.2 and PFPE (C cores) 6.2.
RNA Quality	Average RQN: FF (A cores) 9.1, FFPE (B cores) 2.8 PFPE (C cores) 4.6 and PFPE (D cores) 5.1	Average RQN: FF (A cores) 8.7, FFPE (B cores) 2.6 and PFPE (C cores) 6.3.
DNA Quantity	FF (A cores) 0.6 µg, FFPE (B cores) 0.8 µg, PFPE (C cores) 1.1 µg and PFPE (D cores) 1.4 µg per 6.0 mm^3 tissue volume Per nucleus (not done)	FF (A cores) 1.3 µg, FFPE (B cores) 2.8 µg and PFPE (C cores) 2.7 µg per 6.2 mm^3 tissue volume FF 0.41 pg, FFPE 0.69 pg and PFPE 0.78 pg per nucleus

RNA Quantity	FF (A cores) 5.2 µg, FFPE (B cores) 2.7 µg, PFPE (C cores) 4.9 µg and PFPE (D cores) 5.4 µg per 6.0 mm^3 tissue volume Per nucleus (not done)	FF (A cores) 4.3 µg, FFPE (B cores) 3.7 µg and PFPE (C cores) 7.8 µg per 6.2 mm^3 tissue volume FF 1.40 pg, FFPE 0.94 pg and PFPE 2.24 pg per nucleus

Supplemental Table 2. Pathos DELTA tissue processing protocol for formalin-fixed B cores in the 3-core and 4-core studies.

Phase	Phase Name	Reagent	Phase type	Heating	Vacuum	Step	Time h:min	Temp	Pressure
1	Fixation	Formalin	Fixation	MW and resistance	no	1	0:30	40C	-
						2	0:45	40C	-
						3	0:30	50C	-
						4	0:45	50C	-
2	Flushing	Flushing Mix (~70% Ethanol)	Flushing	no	no	1	0:05	-	-
3	Rinsing1	Ethanol	Rinsing	MW and resistance	no	1	0:10	40C	-
4	Rinsing2	Ethanol	Rinsing	MW and resistance	no	1	0:10	40C	-
						2	0:05	40C	-
5	Ethanol	Ethanol	Dehydration, clearing, other	MW and resistance	no	1	0:20	55C	-
						2	1:50	55C	-
6	Isopropanol	Isopropanol	Dehydration, clearing, other	MW and resistance	no	1	0:20	65C	-
						2	3:40	65C	-
7	Isopropanol2	Isopropanol2	Dehydration, clearing, other	MW and resistance	no	1	0:20	65C	-
						2	0:40	65C	-
						3	0:20	68C	
						4	3:10	68C	-
8	Vaporization	-	Vaporization	no	yes	1	0:03	-	600 mbar
9	Wax impregnation	Wax	Wax	Only resistance	yes	1	0:30	70C	500 mbar
						2	0:20	70C	400 mbar
						3	0:20	70C	300 mbar
						4	0:20	70C	200 mbar
						5	0:20	70C	150 mbar

						6	4:00	65C	100 mbar
						7	3:00	65C	800 mbar

Supplemental Table 3. Citadel 2000 (69810051 Issue 18) tissue processing protocol for PAXgene-fixed C cores in the 4-core study.

Step	Solution	Time h:min	Temp
1	Ethanol 80%	0:30	RT
2	Ethanol 96%	0:30	RT
3	Ethanol 96%	0:30	RT
4	Ethanol 100%	1:00	RT
5	Ethanol 100%	1:00	RT
6	Xylene	1:00	RT
7	Xylene	1:30	RT
8	Histowax	1:15	60°C
9	Histowax	1:15	60°C

Supplemental Table 4. Pathos DELTA tissue processing protocol for PAXgene-fixed D cores in the 4-core study.

Phase	Phase Name	Reagent	Phase type	Heating	Vacuum	Step	Time h:min	Temp	Pressure
1	80% EtOH	80% Ethanol	Dehydration, clearing other	no	no	1	0:30	-	-
2	96% EtOH1	96% Ethanol1	Dehydration, clearing other	no	no	1	0:30	-	-
3	96% EtOH2	96% Ethanol2	Dehydration, clearing other	no	no	1	0:30	-	-
4	100% Ethanol1	Ethanol (ABS)1	Dehydration, clearing other	no	no	1	1:00	-	-
5	100% Ethanol2	Ethanol (ABS)2	Dehydration, clearing other	no	no	1	1:00	-	-
6	Xylene1	Xylene1	Dehydration, clearing other	no	no	1	1:00	-	-
7	Xylene2	Xylene2	Dehydration, clearing other	no	no	1	1:30	-	-
8	Wax impregnation	Wax	Wax	Only resistance	no	1	2:30	60C	-

Supplemental Table 5. Leica TP1020 tissue processing protocol for PAXgene-fixed C cores in the 3-core study.

Station	Solution	Time h:min	Temp	Vacuum	Volume of liquid
1	PAXgene Stabilizer	0:05	RT	off	1 liter

2	Ethanol 80%	0:30	RT	on	1 liter
3	Ethanol 90%	1:00	RT	on	1 liter
4	Ethanol 99%	1:00	RT	on	1 liter
5	Ethanol 99%	1:00	RT	on	1 liter
6	Isopropanol	1:00	RT	on	1 liter
7	Isopropanol	1:00	RT	on	1 liter
8	Xylene	1:00	RT	on	1 liter
9	Xylene	1:00	RT	on	1 liter
10	Xylene/ParaplastXtra 50:50	1:00	50°C	on	1 liter (500 ml + 500 ml)
11	Paraplast Xtra	1:00	56°C	on	1 liter
12	Paraplast Xtra	1:30	56°C	on	1 liter

Supplemental Table 6. BioMediTech H&E staining protocol for FFPE B and donor macro sections, and PFPE C and D cores in 4-core study.

Step	**Reagent**	**Producer, Cat no**	**Time min:sec**
1	Hexane		3:00
2	Hexane		3:00
3	ABS EtOH		2:00
4	ABS EtOH		1:00
5	94% EtOH		2:00
6	70% EtOH		1:00
7	dH2O	MilliQ-distilled H2O	0:30
8	Hematoxylin	Mayers HTX Histolab, Histolab Products AB, Cat No 01820	14:00
9	H2O		7:00
10	dH2O	MilliQ-distilled H2O	0:40
11	Eosin	Eosin 0,2% Histolab, Histolab Products AB, Cat No 01650	1:30
12	H2O		1:00
13	dH2O	MilliQ-distilled H2O	0:30
14	94% EtOH		2:00
15	ABS EtOH		2:00
16	ABS EtOH		2:00
17	ABS EtOH		2:00
18	Xylene		2:00

Supplemental Table 7. BioMediTech H&E staining protocol for FF A cores in 4-core study.

Step	**Reagent**	**Producer, Cat no**	**Time min:sec**
1	dH2O	MilliQ-distilled H2O	0:30

2	Hematoxylin	Mayers HTX Histolab, Histolab Products AB, Cat No 01820	6:00
3	H2O		7:00
4	dH2O	MilliQ-distilled H2O	0:40
5	Eosin	Eosin 0,2% Histolab, Histolab Products AB, Cat No 01650	2:00
6	H2O		1:00
7	dH2O	MilliQ-distilled H2O	0:30
8	94% EtOH		2:00
9	94% EtOH		2:00
10	ABS EtOH		1:00
11	ABS EtOH		2:00
12	ABS EtOH		2:00
13	Xylene		2:00

Supplemental Table 8. Fimlab pathology laboratory H&E staining protocol for FFPE B cores in 3-core study

Step	**Reagent**	**Producer, Cat no**	**Time min:sec**
1	HistoClear II 1	National diagnostics, HS-202	3:00
2	HistoClear II 2	National diagnostics, HS-202	3:00
3	96% EtOH 1		0:10
4	96% EtOH 2		2:00
5	70% EtOH		2:00
6	Running tap water		1:00
7	Hematoxylin	Dako, CS700	0:45
8	dH20	MilliQ-distilled H2O	1:00
9	Bluing Buffer	Dako, CS702	1:00
10	Running tap water		1:00
11	70% EtOH 2		1:00
12	Eosin	Dako, CS701	1:00
13	96% EtOH 3		1:00
14	99,9% EtOH 1		1:00
15	99,9% EtOH 2		1:00
16	99,9% EtOH 3		1:00
17	HistoClear II		1:00

Supplemental Table 9. BioMediTech H&E staining protocol for PFPE C cores in 3-core study.

Step	**Reagent**	**Producer, Cat no**	**Time min:sec**
1	HistoClear II 1	National diagnostics, HS-202	3:00

2	HistoClear II 2	National diagnostics, HS-202	3:00
3	96% EtOH 1		0:10
4	96% EtOH 2		2:00
5	70% EtOH		2:00
6	Running tap water		1:00
7	Hematoxylin	Dako, CS700	0:45
8	dH20	MilliQ-distilled H2O	1:00
9	Bluing Buffer	Dako, CS702	1:00
10	Running tap water		1:00
11	70% EtOH 2		1:00
12	Eosin diluted 1:2	Dako, CS701	0:05
13	96% EtOH 3		1:00
14	99,9% EtOH 1		1:00
15	99,9% EtOH 2		1:00
16	99,9% EtOH 3		1:00
17	HistoClear II		1:00

Supplemental Table 10. BioMediTech H&E staining protocol for FF A cores in 3-core study.

Step	Reagent	Producer, Cat no	Time min:sec
1	dH2O	MilliQ-distilled H2O	0:30
2	Hematoxylin	Mayers HTX Histolab, Histolab Products AB, Cat No 01820	10:00
3	H2O		7:00
4	dH2O	MilliQ-distilled H2O	0:40
5	Eosin diluted 1:2	Eosin 0,2% Histolab, Histolab Products AB, Cat No 01650	0:30
6	H2O		1:00
7	dH2O	MilliQ-distilled H2O	0:30
8	94% EtOH		2:00
9	94% EtOH		2:00
10	ABS EtOH		1:00
11	ABS EtOH		2:00
12	ABS EtOH		2:00
13	Xylene		2:00

Supplemental Table 11. DNA MiSeq assay target list

Gene	Total size of targeted region (bp)
AR	186608
HES6	755
TP53	1503
PTEN	1392
SMAD4	1879
MYC	1425
FOXA1	1459
KDM5B	5175
CHD4	6519

KMT2C	15916
CTNNB1	2626
HOXB13	895
SPOP	1305
MED12	7434
AKT1	1703
KRAS	787
EVC	3399
TMEM33	884
NPFFR2	1671
MYOZ2	895
SPOCK3	1607
SMPD1	2016
FSHB	430
FOLR2	848
MMP7	924
CRTAM	1382
CYFIP1	4743
EXD1	1745
LIPC	1680
ALPK3	6004
SYNM	4777
FEM1A	2030
JUND	1064
CEBPG	473
FOSB	1097
SYT3	1933

HES6	2037
ACPP	3807
SKIL	7498
SPINK1	1478
FKBP5	10628
SGK1	6967
ETV1	8401
MSMB	1860
FLI1	4849
ASCL1	2472
CHGA	2194
ETV4	3095
HPN	2677
KLK3	2321
ERG	7498
TMPRSS2	5418
SYP	3377
AR	11810

Supplemental Table 12. RNA MiSeq assay Target List

Gene	Transcript length (bp)
TBP	2038
DDX1	2988
STARD7	3422
SLC45A3	3702

Supplemental Table 13. Summary of nucleus counts in the 3-core study.

		FF (A cores)	FFPE (B cores)	PFPE (C cores)
Number of nuclei per standard slide	Mean	79839	98609	86892
	SD	15255	19214	19756
	Median	75664	94343	81995
Estimated number of nuclei per 6.2 mm^3 tissue	Mean	3.08×10^6	4.01×10^6	3.54×10^6
	SD	588825	782008	804064
	Median	2.92×10^6	3.84×10^6	3.34×10^6